

Shield Synthesis for LTL Modulo Theories

Andoni Rodríguez^{1,2}, Guy Amir³, Davide Corsi⁴, César Sánchez¹, Guy Katz³

¹IMDEA Software Institute, Spain

²Universidad Politécnica de Madrid, Spain

³The Hebrew University of Jerusalem, Israel

⁴University of California, Irvine, USA

Abstract

In recent years, Machine Learning (ML) models have achieved remarkable success in various domains. However, these models also tend to demonstrate unsafe behaviors, precluding their deployment in safety-critical systems. To cope with this issue, ample research focuses on developing methods that guarantee the safe behaviour of a given ML model. A prominent example is *shielding* which incorporates an external component (a “shield”) that blocks unwanted behavior. Despite significant progress, shielding suffers from a main setback: it is currently geared towards properties encoded solely in propositional logics (e.g., LTL) and is unsuitable for richer logics. This, in turn, limits the widespread applicability of shielding in many real-world systems. In this work, we address this gap, and extend shielding to LTL modulo theories, by building upon recent advances in reactive synthesis modulo theories. This allowed us to develop a novel approach for generating shields conforming to complex safety specifications in these more expressive, logics. We evaluated our shields and demonstrate their ability to handle rich data with temporal dynamics. To the best of our knowledge, this is the first approach for synthesizing shields for such expressivity.

1 Introduction

Recently, DNN-based agents trained using Deep Reinforcement Learning (DRL) have been shown to successfully control reactive systems of high complexity (e.g., (Marchesini and Farinelli 2020)), such as robotic platforms. However, despite their success, DRL controllers still suffer from various safety issues; e.g., small perturbations to their inputs, resulting either from noise or from a malicious adversary, can cause even state-of-the-art agents to react unexpectedly (e.g., (Goodfellow, Shlens, and Szegedy 2014)). This issue raises severe concerns regarding the deployment of DRL-based agents in safety-critical reactive systems.

In order to cope with these DNN reliability concerns, the formal methods community has recently put forth various tools and techniques that rigorously ensure the safe behaviour of DNNs (e.g., (Katz et al. 2017)), and specifically, of DRL-controlled reactive systems (e.g., (Bassan et al. 2023)). One of the main approaches that is gaining popularity, is *shielding* (Bloem et al. 2015; Alshiekh et al. 2018), i.e., the incorporation of an external component (a “shield”) that *forces* an agent to behave safely according to a given specification. This specification φ is usually expressed as

a propositional formula, in which the atomic propositions represent the inputs (I) and outputs (O) of the system, controlled by the DNN in question. Once φ is available, shielding seeks to guarantee that *all* behaviors of the given system D satisfy φ through the means of a shield S : whenever the system encounters an input I that triggers an erroneous output (i.e., $O : D(I)$ for which $\varphi(I, O)$ does not hold), S corrects O and replaces it with another action O' , to ensure that $\varphi(I, O')$ does hold. Thus, the combined system $D \cdot S$ never violates φ . Shields are appealing for multiple reasons: they do not require “white box” access to D , a single shield S can be used for multiple variants of D , it is usually computationally cheaper than static methods like DNN verification etc. Moreover, shields are intuitive for practitioners, since they are synthesized based on the required φ . However, despite significant progress, modern shielding methods still suffer from a main setback: they are only applicable to specifications in which the inputs/outputs are over Boolean atomic propositions. This allows users to encode only discrete specifications, typically in *Linear Temporal Logic* (LTL). Thus, as most real-world systems rely on rich data specifications, this precludes the use of shielding in various such domains, such as continuous input spaces.

In this work, we address this gap and present a novel approach for shield synthesis that makes use of LTL modulo theories ($LTL_{\mathcal{T}}$), where Boolean propositions are extended to literals from a (multi-sorted) first-order theory \mathcal{T} . Concretely, we leverage Boolean abstraction methods (Rodríguez and Sánchez 2023), which transform $LTL_{\mathcal{T}}$ specifications into equi-realizable pure (Boolean) LTL specifications. We combine Boolean abstraction with reactive $LTL_{\mathcal{T}}$ synthesis (Rodríguez and Sánchez 2024b), extending the common LTL shielding theory into a $LTL_{\mathcal{T}}$ shielding theory. Using $LTL_{\mathcal{T}}$ shielding, we are able to construct shields for more expressive specifications. This, in turn, allows us to override unwanted actions in a (possibly infinite) domain of \mathcal{T} , and guarantee the safety of DNN-controlled systems in such complex scenarios. In summary, our contributions are: (1) developing two methods for shield synthesis over $LTL_{\mathcal{T}}$ and presenting their proof of correctness; (2) an analysis of the impact of the Boolean abstractions in the precision of shields; (3) a formalization of how to construct optimal shields using objective functions; and (4) an empirical evaluation that shows the applicability of our techniques.

2 Preliminaries

LTL and LTL \mathcal{T} . We start from LTL (Pnueli 1977; Manna and Pnueli 1995), which has the following syntax:

$$\varphi ::= \top \mid a \mid \varphi \vee \varphi \mid \neg \varphi \mid \bigcirc \varphi \mid \varphi \mathcal{U} \varphi,$$

where $a \in \text{AP}$ is an *atomic proposition*, $\{\wedge, \neg\}$ are the common Boolean operators of *conjunction* and *negation*, respectively, and $\{\bigcirc, \mathcal{U}\}$ are the *next* and *until* temporal operators, respectively. Additional temporal operators include \mathcal{R} (*release*), \diamond (*finally*), and \square (*always*), which can be derived from the syntax above. Given a set of atomic propositions \bar{a} we use $\text{val}(\bar{a})$ for a set of possible valuations of variables in \bar{a} (i.e. $\text{val}(\bar{a}) = 2^{\bar{a}}$), and we use $v_{\bar{a}}$ to range over $\text{val}(\bar{a})$. We use $\Sigma = \text{val}(\text{AP})$. The semantics of LTL formulas associates traces $\sigma \in \Sigma^\omega$ with LTL fomulas (where $\sigma \models \top$ always holds, and \vee and \neg are standard):

$$\begin{aligned} \sigma \models a & \quad \text{iff } a \in \sigma(0) \\ \sigma \models \bigcirc \varphi & \quad \text{iff } \sigma^1 \models \varphi \\ \sigma \models \varphi_1 \mathcal{U} \varphi_2 & \quad \text{iff for some } i \geq 0 \ \sigma^i \models \varphi_2, \text{ and} \\ & \quad \text{for all for all } 0 \leq j < i, \sigma^j \models \varphi_1 \end{aligned}$$

A safety formula φ is such that for every failing trace $\sigma \not\models \varphi$ there is a finite prefix u of σ , such that all σ' extending u also falsify φ (i.e. $\sigma' \not\models \varphi$).

The syntax of LTL modulo theory (LTL \mathcal{T}) replaces atoms a by literals l from some theory \mathcal{T} . Even though we use multi-sorted theories, for clarity of explanation we assume that \mathcal{T} has only one sort and use \mathbb{D} for the domain, the set that populates the sort of its variables. For example, the domain of linear integer arithmetic $\mathcal{T}_{\mathbb{Z}}$ is \mathbb{Z} and we denote this by $\mathbb{D}(\mathcal{T}_{\mathbb{Z}}) = \mathbb{Z}$. Given an LTL \mathcal{T} formula $\varphi(\bar{z})$ with variables \bar{z} the semantics of LTL \mathcal{T} now associate traces σ (where each letter is a valuation of \bar{z} , i.e., a mapping from \bar{z} into \mathbb{D}) with LTL \mathcal{T} formulae. The semantics of the Boolean and temporal operators are as in LTL, and for literals:

$$\sigma \models l \text{ iff the valuation } \sigma(0) \text{ of } \bar{z} \text{ makes } l \text{ true according to } \mathcal{T}$$

The Synthesis Problem. Reactive LTL synthesis (Thomas 2008; Piterman, Pnueli, and Sa’ar 2006) is the task of producing a system that satisfies a given LTL specification φ , where atomic propositions in φ are split into variables controlled by the environment (“input variables”) and by the system (“output variables”), denoted by \bar{e} and \bar{s} , respectively. Synthesis corresponds to a game where, in each turn, the environment player produces values for the input propositions, and the system player responds with values of the output propositions. A play is an infinite sequence of turns, i.e., an infinite interaction of the system with the environment. A strategy for the system is a tuple $C_{\mathbb{B}} : \langle Q, q_0, \delta, o \rangle$ where Q is a finite set of states, $q_0 \in Q$ is the initial state, $\delta : Q \times \text{val}(\bar{e}) \rightarrow Q$ is the transition function and $o : Q \times \text{val}(\bar{e}) \rightarrow \text{val}(\bar{s})$ is the output function. $C_{\mathbb{B}}$ is said to be *winning* for the system if all the possible plays played according to the strategy satisfy the LTL formula $\varphi_{\mathbb{B}}$. In this paper we use “strategy” and “controller” interchangeably.

We also introduce the notion of *winning region* (WR), which encompasses all possible winning moves for the system in safety formulae. A winning region $WR : \langle Q, I, T \rangle$ is

a tuple where Q is a finite set of states, $I \subseteq Q$ is a set of initial states and $T : Q \times \text{val}(\bar{e}) \rightarrow 2^{(Q \times \text{val}(\bar{s}))}$ is the transition relation, which provides for a given state q and input $v_{\bar{e}}$, all the possible pairs of legal successor and output $(q', v_{\bar{s}})$. For a safety specification, every winning strategy is “included” into the WR (i.e., there is an embedding map). LTL realizability is the decision problem of whether there is a winning strategy for the system (i.e., check whether $WR \neq \emptyset$), while LTL synthesis is the computational problem of producing one.

However, in LTL \mathcal{T} synthesis (Rodríguez and Sanchez 2023; Rodríguez and Sánchez 2024b), the specification is expressed in a richer logic where propositions are replaced by literals from some \mathcal{T} . In LTL \mathcal{T} the (first order) variables in specification $\varphi_{\mathcal{T}}$ are still split into those controlled by the environment (\bar{x}), and those controlled by the system (\bar{y}), where $\bar{x} \cap \bar{y} = \emptyset$. We use $\varphi_{\mathcal{T}}(\bar{x}, \bar{y})$ to emphasize that $\bar{x} \cup \bar{y}$ are all the variables occurring in $\varphi_{\mathcal{T}}$. The alphabet is now $\Sigma_{\mathcal{T}} = \text{val}(\bar{x} \cup \bar{y})$ (note that now valuations map a variable x to $\mathbb{D}(\mathcal{T})$). We denote by $t[\bar{x} \leftarrow v_{\bar{x}}]$, the substitution in t of variables \bar{x} by values $v_{\bar{x}}$ (similarly for $t[\bar{y} \leftarrow v_{\bar{y}}]$), and also $t[\bar{e} \leftarrow v_{\bar{e}}]$ and $t[\bar{s} \leftarrow v_{\bar{s}}]$ for Boolean variables (propositions). A trace π is an infinite sequence of valuations in $\mathbb{D}(\mathcal{T})$, which induces an infinite sequence of Boolean values of the literals occurring in $\varphi_{\mathcal{T}}$ and, in turn, an evaluation of $\varphi_{\mathcal{T}}$ using the semantics of the temporal operators. For example, given $\psi = \square(y < x)$ the trace $\pi \{(x : 2, y : 6), (x : 15, y : 27) \dots\}$ induces $\{\text{false}, \text{true}\} \dots$. We use π_x to denote the projection of π to the values of only x (resp. π_y for y). A strategy or controller for the system in \mathcal{T} is now a tuple $C_{\mathcal{T}} : \langle Q, q_0, \delta, o \rangle$ where Q and $q_0 \in Q$ are as before, and $\delta : Q \times \text{val}(\bar{x}) \rightarrow Q$ and $o : Q \times \text{val}(\bar{x}) \rightarrow \text{val}(\bar{y})$.

Boolean Abstraction. Boolean abstraction (Rodríguez and Sánchez 2023) transforms an LTL \mathcal{T} specification $\varphi_{\mathcal{T}}$ into an LTL specification $\varphi_{\mathbb{B}}$ in the same temporal fragment (e.g., safety to safety) that preserves realizability, i.e., $\varphi_{\mathcal{T}}$ and $\varphi_{\mathbb{B}}$ are *equi-realizable*. Then, $\varphi_{\mathbb{B}}$ can be fed into an off-the-shelf synthesis engine, which generates a controller or a WR for realizable instances. Boolean abstraction transforms $\varphi_{\mathcal{T}}$, which contains literals l_i , into $\varphi_{\mathbb{B}} = \varphi_{\mathcal{T}}[l_i \leftarrow s_i] \wedge \varphi^{\text{extra}}$, where $\bar{s} = \{s_i \mid \text{for each } l_i\}$ is a set of fresh atomic propositions controlled by the system—such that s_i replaces l_i —and where φ^{extra} is an additional sub-formula that captures the dependencies between the \bar{s} variables. The formula φ^{extra} also includes additional variables \bar{e} (controlled by the environment) that encode that the environment can leave the system with the power to choose certain valuations of the variables \bar{s} .

We often represent a valuation $v_{\bar{s}}$ of the Boolean variables \bar{s} (which map each variable in \bar{s} to *true* or *false*) as a *choice* c (an element of $2^{\bar{s}}$), where $s_i \in c$ means that $v_{\bar{s}}(s_i) = \text{true}$. The characteristic formula $f_c(\bar{x}, \bar{y})$ of a choice c is $f_c = \bigwedge_{s_i \in c} l_i \wedge \bigwedge_{s_i \notin c} \neg l_i$. We use \mathcal{C} for the set of choices, i.e., sets of sets of \bar{s} . A *reaction* $r \subset \mathcal{C}$ is a set of choices, which characterizes the possible responses of the system as the result to a move of the environment. The *characteristic formula* $f_r(\bar{x})$ of a reaction r is:

$(\bigwedge_{c \in r} \exists \bar{y}. f_c) \wedge (\bigwedge_{c \notin r} \forall \bar{y}. \neg f_c)$. We say that r is a valid reaction whenever $\exists \bar{x}. f_r(\bar{x})$ is valid. Intuitively, f_r states that for some $v_{\bar{x}}$ by the environment, the system can respond with $v_{\bar{y}}$ making the literals in some choice $c \in r$ but cannot respond with $v_{\bar{y}}$ making the literals in choices $c \notin r$. The set VR of valid reactions partitions precisely the moves of the environment in terms of the reaction power left to the system. For each valid reaction r there is a fresh environment variable $e \in \bar{e}$ used in φ^{extra} to capture the move of the environment that chooses reaction r . The formula $f_r(\bar{x})[\bar{x} \leftarrow v_{\bar{x}}]$ is true if a given valuation $v_{\bar{x}}$ of \bar{x} is one move of the environment characterized by r . The formula φ^{extra} also constrains the environment such that exactly one of the variables in \bar{e} is true, which forces that the environment chooses precisely one valid reaction r when the variable e that corresponds to r is true.

Example 1 (Running example and abstraction). Let $\varphi_{\mathcal{T}} = \square(R_0 \wedge R_1)$ where:

$$R_0 : (x < 10) \rightarrow \bigcirc(y > 9) \quad R_1 : (x \geq 10) \rightarrow (y \leq x),$$

where $\bar{x} = \{x\}$ is controlled by the environment and $\bar{y} = \{y\}$ by the system. In integer theory $\mathcal{T}_{\mathbb{Z}}$ this specification is realizable (consider the strategy to always play $y : 10$) and the Boolean abstraction first introduces s_0 to abstract $(x < 10)$, s_1 to abstract $(y > 9)$ and s_2 to abstract $(y \leq x)$. Then $\varphi_{\mathbb{B}} = \varphi'' \wedge \square(\varphi^{legal} \rightarrow \varphi^{extra})$ where $\varphi'' = (s_0 \rightarrow \bigcirc s_1) \wedge (\neg s_0 \rightarrow s_2)$ is a direct abstraction of $\varphi_{\mathcal{T}}$. Finally, φ^{extra} captures the dependencies between the abstracted variables:

$$\varphi^{extra} : \left(\begin{array}{l} (e_0 \rightarrow (f_{c_1} \vee f_{c_2})) \\ \wedge (e_{0+} \rightarrow (f_{c_1} \vee f_{c_2} \vee f_{c_3})) \\ \wedge (e_1 \rightarrow (f_{c_4} \vee f_{c_5} \vee f_{c_6})) \end{array} \right),$$

where $f_{c_1} = (s_0 \wedge s_1 \wedge \neg s_2)$, $f_{c_2} = (s_0 \wedge \neg s_1 \wedge s_2)$, $f_{c_3} = (s_0 \wedge \neg s_1 \wedge \neg s_2)$, $f_{c_4} = (\neg s_0 \wedge s_1 \wedge s_2)$, $f_{c_5} = (s_0 \wedge s_1 \wedge \neg s_2)$ and $f_{c_6} = (\neg s_0 \wedge \neg s_1 \wedge s_2)$ and where $c_0 = \{s_0, s_1, s_2\}$, $c_1 = \{s_0, s_1\}$, $c_2 = \{s_0, s_2\}$, $c_3 = \{s_0\}$, $c_4 = \{s_1, s_2\}$, $c_5 = \{s_1\}$, $c_6 = \{s_1\}$ and $c_7 = \emptyset$. Also, $\bar{e} = \{e_0, e_{0+}, e_1\}$ belong to the environment and represent $(x < 10)$, $(x < 9)$ ¹ and $(x \geq 10)$, respectively. $\varphi^{legal} : (e_0 \wedge \neg e_1 \wedge \neg e_2) \vee (\neg e_0 \wedge e_1 \wedge \neg e_2) \vee (\neg e_0 \wedge \neg e_1 \wedge e_2)$ encodes that \bar{e} characterizes a partition of the (infinite) input valuations of the environment and that only one of the \bar{e} is true in every move; e.g., the valuation $v_{\bar{e}} : \langle e_0 : \text{false}, e_0^+ : \text{true}, e_1 : \text{false} \rangle$ of \bar{e} corresponds to the choice of the environment where only e_0^+ is true (and we use $v_{\bar{e}} : e_0^+$ for a shorter notation). Subformulae such as $(\neg s_0 \wedge s_1 \wedge s_2)$ represent the choices of the system (in this case, $c = \{s_1, s_2\}$), that is, given a decision of the environment (a valuation of \bar{e} that makes exactly one variable $e \in \bar{e}$ true), the system can react with one of the choices c in the disjunction implied by e . Note that $f_c = \neg(x < 2) \wedge (y > 1) \wedge (y \leq x)$. Also, note that c can be represented as $v_{\bar{s}} : \langle s_0 : \text{false}, s_1 : \text{true}, s_2 : \text{true} \rangle$.

¹We address implications of $(x < 9)$ being subsumed by $(x < 10)$ in Subsec. 3.2.

3 Shielding with LTL Modulo Theories

In shielding, at every step, the external design D —e.g., a DRL sub-system—produces an output $v_{\bar{s}}$ from a given input $v_{\bar{e}}$ provided by the environment. The pair $(v_{\bar{e}}, v_{\bar{s}})$ is passed to the shield S which decides, at every step, whether $v_{\bar{s}}$ proposed by D is safe with respect to some specification φ . The combined system $D \cdot S$ is guaranteed to satisfy φ . Using $\text{LTL}_{\mathcal{T}}$ we can define richer properties than in propositional LTL (which has been previously used in shielding). For instance, consider a classic $D \cdot S$ context in which the D is a robotic navigation platform and $\varphi : \square(\text{LEFT} \rightarrow \bigcirc \neg \text{LEFT})$. Then, if D chooses to turn LEFT after a LEFT action, the shield will consider this second action to be dangerous, and will override it with e.g., RIGHT. If $\text{LTL}_{\mathcal{T}}$ is used instead of LTL, specifications can be more sophisticated including, for example, numeric data.

Shielding modulo theories is the problem of building a shield $S_{\mathcal{T}}$ from a specification $\varphi_{\mathcal{T}}$ in which at least one of the input variables \bar{x} or one of the output variables \bar{y} are not Boolean.

A shield $S_{\mathcal{T}}$ conforming to $\varphi_{\mathcal{T}}$ will evaluate if a pair $(\bar{x} : v_{\bar{x}}, \bar{y} : v_{\bar{y}})$ violates $\varphi_{\mathcal{T}}$ and propose an overriding output $\bar{y}' : v_{\bar{y}}'$ if so. This way, $D \cdot S_{\mathcal{T}}$ never violates $\varphi_{\mathcal{T}}$. Note that it is possible that $\varphi_{\mathcal{T}}$ is unrealizable, which means that some environment plays will inevitably lead to violations, and hence $S_{\mathcal{T}}$ cannot be constructed, because $\text{WR} = \emptyset$.

Example 2 (Running example as shield). Recall $\varphi_{\mathcal{T}}$ from Ex. 1. Also, consider D receives an input trace $\pi_x = \langle 15, 15, 7, 5, 10 \rangle$, and produces the output trace $\pi_y = \langle 6, 5, 13, 16, 11 \rangle$. We can see D violates $\varphi_{\mathcal{T}}$ in the fifth step, since $(x < 10)$ holds in fourth step (so v_y has to be such that $(y : v_y > 9)$ in the fourth step and $(v_y : \leq 10)$ must hold in the fifth step) but $(y : 11 \leq 10)$ is not true. Instead, a $S_{\mathcal{T}}$ conforming to $\varphi_{\mathcal{T}}$ would notice that $(x : 10, y : 11)$ violates $\varphi_{\mathcal{T}}$ in this fifth step and would override v_y with v_y' to produce $(y' : 10)$, which is the only possible valuation of y' that does not violate $\varphi_{\mathcal{T}}$. Note that $S_{\mathcal{T}}$ did not intervene in the remaining steps. Thus, $D \cdot S_{\mathcal{T}}$ satisfies $\varphi_{\mathcal{T}}$ in the example.

3.1 $\text{LTL}_{\mathcal{T}}$ Shield Construction

We propose two different architectures for $S_{\mathcal{T}}$: one following a deterministic strategy and another one that is non-deterministic. Both start from $\varphi_{\mathcal{T}}$ and use Boolean abstraction as the core for the temporal information, but they vary on the way to detect erroneous outputs from D and how to provide corrections.

Shields as Controllers. The first method leverages $\text{LTL}_{\mathcal{T}}$ controller synthesis (see Fig. 1(a)) together with a component to detect errors in D . The process is as follows, starting from a specification $\varphi_{\mathcal{T}}$:

1. Boolean abstraction (Rodríguez and Sánchez 2023) transforms $\varphi_{\mathcal{T}}$ into an equi-realizable LTL $\varphi_{\mathbb{B}}$.
2. A Boolean controller $C_{\mathbb{B}}$ is synthesized from $\varphi_{\mathbb{B}}$ (using e.g., (Meyer, Sickert, and Luttenberger 2018)). $C_{\mathbb{B}}$ receives Boolean inputs $v_{\bar{e}}$ and provides Boolean outputs $v_{\bar{s}}$.

3. We synthesize a richer controller $C_{\mathcal{T}}$ that receives $v_{\bar{x}}$ and produces outputs $v'_{\bar{y}}$ in $\mathbb{D}(\mathcal{T})$. Note the apostrophe in $v'_{\bar{y}}$, since $v_{\bar{y}}$ is the output of D .
4. $S_{\mathcal{T}}$ receives the output $v_{\bar{y}}$ provided by D and checks if the pair $(v_{\bar{x}}, v_{\bar{y}})$ violates $\varphi_{\mathcal{T}}$: if there is a violation, it overrides $v_{\bar{y}}$ with $v'_{\bar{y}}$; otherwise, it permits $v_{\bar{y}}$.

We now elaborate on the last steps. To construct $C_{\mathcal{T}}$ from $C_{\mathbb{B}}$ we use (Rodríguez and Sanchez 2023; Rodríguez and Sánchez 2024b), where $C_{\mathcal{T}}$ is composed of three sub-components:

- A **partitioner** function, which computes Boolean inputs $v_{\bar{e}}$ from the richer inputs $v_{\bar{x}}$ via partitioning, checking whether $f_r(v_{\bar{x}})$ is true. Recall that every $v_{\bar{x}}$ is guaranteed to belong to exactly one reaction r .
- A **Boolean controller** $C_{\mathbb{B}}$, which receives $v_{\bar{e}}$ and provides Boolean outputs $v_{\bar{s}}$. Also recall that each Boolean variable in $v_{\bar{s}}$ corresponds exactly to a literal in $\varphi_{\mathcal{T}}$ and that f_c is the characteristic formula of c .
- A **provider**, which computes an output $v'_{\bar{y}}$ from f_c and r such that $v'_{\bar{y}}$ is a model² of the formula $\exists y'. (f_r(\bar{x}) \rightarrow f_c(\bar{y}', \bar{x}))[\bar{x} \leftarrow v_{\bar{x}}]$.

The composition of the **partitioner**, $C_{\mathbb{B}}$ and the **provider** implements $C_{\mathcal{T}}$ (see (Rodríguez and Sanchez 2023; Rodríguez and Sánchez 2024b)). For each of these components g , let us denote with $g(t_0) = t_1$ the application of g with input t_0 . Then, the following holds:

Lemma 1. *Let $\varphi_{\mathcal{T}}$ be an LTL $_{\mathcal{T}}$ specification, $\varphi_{\mathbb{B}}$ its equi-realizable Boolean abstraction and $C_{\mathbb{B}}$ a controller for $\varphi_{\mathbb{B}}$. Let q be a state of $C_{\mathbb{B}}$ after processing inputs $v_{\bar{x}}^0 \dots v_{\bar{x}}^n$, and let $v_{\bar{x}}$ be the next input from the environment. Let **partitioner** $(v_{\bar{x}}) = v_{\bar{e}}$ be the partition corresponding to $v_{\bar{x}}$, $o(q, v_{\bar{e}}) = v_{\bar{s}}$ be the output of $C_{\mathbb{B}}$ and c be the choice associated to $v_{\bar{s}}$. Then, if r is a valid reaction, the formula $\exists \bar{y}. f_r(v_{\bar{x}}) \rightarrow f_c(\bar{y}, v_{\bar{x}})$ is satisfiable in \mathcal{T} , where $c \in r$.*

In other words, $C_{\mathcal{T}}$ never has to face with moves from $C_{\mathbb{B}}$ that cannot be mimicked by **provider** with appropriate values for $v_{\bar{y}}$. Thus, a shield $S_{\mathcal{T}}$ based on $C_{\mathcal{T}}$ (see Fig. 1(a)) first detects whether a valuation pair $(\bar{x} : v_{\bar{x}}, \bar{y} : v_{\bar{y}})$ suggested by D violates $\varphi_{\mathcal{T}}$. To do so, at each time-step, $C_{\mathcal{T}}$ obtains $v_{\bar{s}}$ by $C_{\mathbb{B}}$, with associated c , and it checks whether $f_r(v_{\bar{x}}) \rightarrow f_c(v_{\bar{x}}, v_{\bar{y}})$ is valid, that is, whether the output proposed is equivalent to the move of $C_{\mathbb{B}}$ (in the sense that every literal l_i from $(v_{\bar{x}}, v_{\bar{y}})$ has the same valuation $v_{\bar{s}}$ given by $C_{\mathbb{B}}$). If the formula is valid, then $v_{\bar{y}}$ is maintained. Otherwise, the **provider** is invoked to compute a $v'_{\bar{y}}$ that matches the move of $C_{\mathbb{B}}$. In both cases, $S_{\mathcal{T}}$ guarantees that $v_{\bar{s}}$ remains unaltered in $C_{\mathbb{B}}$ and therefore $\varphi_{\mathcal{T}}$ is guaranteed. For instance, in the hypothetical simplistic case where $f_r = \text{true}$, and consider that $C_{\mathbb{B}}$ outputs a $v_{\bar{s}}$ with associated

²In this paper we implement the calculation of $v'_{\bar{y}}$ using SMT solving (concretely, Z3 (de Moura and Björner 2008)). An alternative is to statically use functional synthesis (such as AEVAL (Fedyukovich, Gurfinkel, and Gupta 2019) for $\forall^* \exists^*$ formulae), which we study in detail in a companion paper and which does not allow optimization using soft constraints in Subsec. 3.3.

c such that $f_c(x, y) = (y > 2) \wedge (x < y)$ in $\mathcal{T}_{\bar{z}}$. Then if the input is $x : 5$, a candidate output $y : 4$ of D would result in $f_r(5) \rightarrow f_c(5, 4) = (4 > 2) \wedge (5 < 4)$, which does not hold. Thus, $y : 4$ must be overridden, so $S_{\mathcal{T}}$ will return a model of $\exists y'. f_r(x) \rightarrow (y' > 2) \wedge (x < y')[x \leftarrow 5]$. One such possibility is $y' : 6$.

Lemma 2. *Let $\varphi_{\mathbb{B}}$ be an equi-realizable abstraction of $\varphi_{\mathcal{T}}$, $C_{\mathbb{B}}$ a controller for $\varphi_{\mathbb{B}}$ and $C_{\mathcal{T}}$ a corresponding controller for $\varphi_{\mathcal{T}}$. Also, consider input $v_{\bar{x}}$ and output $v_{\bar{y}}$ by D and $v'_{\bar{y}}$ by **provider** of $C_{\mathcal{T}}$. If both $f_r(v_{\bar{x}}) \rightarrow f_c(v_{\bar{x}}, v_{\bar{y}})$ and $f_r(v_{\bar{x}}) \rightarrow f_c(v_{\bar{x}}, v'_{\bar{y}})$ hold, then $v_{\bar{y}}$ and $v'_{\bar{y}}$ correspond to the same move of $C_{\mathbb{B}}$.*

In other words, if $v_{\bar{y}}$ and $v'_{\bar{y}}$ make the same literals true, a shield $S_{\mathcal{T}}$ based on $C_{\mathcal{T}}$ will not override $v_{\bar{y}}$; whereas, otherwise, it will output $v'_{\bar{y}}$.

Theorem 1 (Correctness of $D \cdot S_{\mathcal{T}}$ based on $C_{\mathcal{T}}$). *Let D be an external controller and $S_{\mathcal{T}}$ be a shield constructed from a synthesized $C_{\mathcal{T}}$ from a specification $\varphi_{\mathcal{T}}$. Then, $D \cdot S_{\mathcal{T}}$ is also a controller for $\varphi_{\mathcal{T}}$.*

In other words, given $\varphi_{\mathcal{T}}$, if \mathcal{T} is decidable in the $\exists^* \forall^*$ -fragment (a condition for the Boolean abstraction (Rodríguez and Sánchez 2023)), then, leveraging $C_{\mathcal{T}}$, a shield $S_{\mathcal{T}}$ conforming to $\varphi_{\mathcal{T}}$ can be computed for every external D whose input-output domain is \mathcal{T} .

More Flexible Shields from Winning Regions. $S_{\mathcal{T}}$ based on $C_{\mathcal{T}}$ are sometimes too intrusive in the sense that they can cause unnecessary corrections, because some $(v_{\bar{x}}, v_{\bar{y}})$ may be labelled as a violation when they are not, only because it satisfies a different collection of literals than the ones chosen by the internal controller $C_{\mathbb{B}}$. Given input $v_{\bar{x}}$, the output $v_{\bar{s}}$ provided by $C_{\mathbb{B}}$ and the output $v_{\bar{y}}$ suggest by D , $(v_{\bar{x}}, v_{\bar{y}})$ is considered to be a *dangerous output* (i.e., a potential violation of $\varphi_{\mathcal{T}}$) whenever a $f_r(v_{\bar{x}})$ holds but the $f_c(v_{\bar{x}}, v_{\bar{y}})$ of the c associated to $C_{\mathbb{B}}$ (**partitioner** $(v_{\bar{x}}) = v_{\bar{s}}$) does not hold. Thus, we study now permissive shields $S_{\mathcal{T}}$ with more precise characterizations of unsafe actions.

The *winning region* (WR) (see Sec. 2) is the most general characterization of the winning states and moves for a safety LTL specification. This second construction can be applied to any subset of WR as long as every state has at least one successor for every input (for example, using the combination of a collection of controllers). The process of computing $S_{\mathcal{T}}$ based on a given winning region $W : \langle Q, I, T \rangle$ is as follows (see Fig. 1(b)), which maintains at each instant a set of current states $Q_{now} \subseteq Q$ of W , starting from the initial set of states I .

1. Compute $\varphi_{\mathbb{B}}$ from $\varphi_{\mathcal{T}}$ using abstraction, as before.
2. We compute the winning region W from $\varphi_{\mathbb{B}}$ (e.g., using (Brenquier et al. 2014)).
3. The **partitioner** computes $v_{\bar{e}}$ from the input values $v_{\bar{x}}$; and, given $v_{\bar{y}}$ provided by D , we produce the unique $v_{\bar{s}}$ from $(v_{\bar{x}}, v_{\bar{y}})$ or equivalently $c = \{s_i | l_i(v_{\bar{x}}, v_{\bar{y}}) \text{ holds}\}$. This is computed by component **getchoice** in Fig. 1(b).
4. From some of the current states $q \in Q_{now}$ maintained, we decide whether $\delta(q, v_{\bar{e}})$ has some successor $(q', v_{\bar{s}})$ or

That is, a set of reactions R is feasible if all the reactions in R are valid and it contains at least all minimal reactions. In order to see whether a set of reactions R is below VR or is indeed VR , we need to check two properties.

Definition 2 (Legitimacy and Strict Covering). *Let R be a set of reactions:*

- R is legitimate iff for all $r \in R$, $\exists \bar{x}. f_r(\bar{x})$ is valid.
- R is a strict covering iff $\forall \bar{x}. \bigvee_{r \in R} f_r(\bar{x})$ is valid.

If R is legitimate, then $R \subseteq VR$. If additionally R is a strict covering, then $R = VR$. Strict covering implies that all possible moves of the environment are covered, regardless of whether there are moves that a clever environment will never play because these moves leave more power to the system than better, alternative moves. A *non-strict* covering does not necessarily consider all the possible moves of the environment in the game, but it still considers at least all optimal environment moves. A non-strict covering can be evaluated by checking that with regard to R , for all \bar{x} , the disjunction of the **playable** choices (see $\bigwedge_{c \in r} \exists \bar{y}. f_c$ of f_r in Sec. 2) of its reactions holds.

Definition 3 (Covering). *The playable formula for a reaction r is defined as $f_r^P(\bar{x}) \stackrel{\text{def}}{=} \bigwedge_{c \in r} \exists \bar{y}. f_c(\bar{x}, \bar{y})$. A set of reactions R is covering if and only if $\varphi_{cov}(R) = \forall \bar{x}. \bigvee_{r \in R} f_r^P(\bar{x})$ is valid.*

Note that a playable formula removes from the characteristic formula f_r the sub-formula ($\bigwedge_{c \notin r} \forall \bar{y}. \neg f_c$) that captures that the choices not in r cannot be achieved by any $v_{\bar{y}}$. We can easily check whether a set of reactions R is feasible, as follows. First, R must be legitimate. Second, if $\varphi_{cov}(R)$ is valid, then R contains a subset of valid reactions that makes R covering in the sense that it considers all the “clever” moves for the environment (considering that a move that leaves less playable choices to the system is more clever for the environment).

Theorem 3. *Let R be a feasible set of reactions and let $\varphi_{\mathbb{B}} = \varphi_{\mathcal{T}}[l_i \leftarrow s_i] \wedge \varphi^{extra}(R)$ be the Booleanization of $\varphi_{\mathcal{T}}$ using R . Then, $\varphi_{\mathcal{T}}$ and $\varphi_{\mathbb{B}}$ are equi-realizable.*

Proof. Let $\varphi_{\mathbb{B}}$ created from VR and let $R \subset VR$ be a feasible reaction set. This means that there is $r \in VR \setminus R$ such that there is an $r' \in R$ with $r' \subseteq r$. Consider a play of $\varphi_{\mathbb{B}}$ where the environment plays the move corresponding to r at some point. If the move is replaced by r' , then if the play with r was winning for the environment then the play with r' is also winning for the environment. Therefore, if $\varphi_{\mathbb{B}}$ is winning for the environment, there is a strategy for the environment where r is never played. It follows that the $\varphi'_{\mathbb{B}}$ that results from R is equi-realizable to the $\varphi_{\mathbb{B}}$ that results from VR . \square

Impact of Boolean Abstractions on Permissivity. To obtain an equi-realizable Boolean abstraction, it is not necessary to consider VR , and instead a feasible set is sufficient. The computation of a feasible set is faster, and generates smaller $\varphi_{\mathbb{B}}$ formulae (Rodriguez and Sánchez 2023). However, there is a price to pay in terms of how permissive the shield is. In practice, it regularly happens that the environment plays moves that are not optimal in the sense that other moves would leave less choice to the system.

Example 3. *Recall Ex. 1. Note that a $C_{\mathbb{B}}$ from $\varphi_{\mathbb{B}}$ can respond with f_c of choices for e_0 , e_0^+ and e_1 . Now consider a $\varphi'_{\mathbb{B}}$ that ignores e_0^+ and its eligible f_c . Thus, a $C_{\mathbb{B}}$ from $\varphi'_{\mathbb{B}}$ can only respond with f_c for e_0 and e_1 . For the sake of the argument, consider the input $x : 0$ forces to satisfy f_{c_2} in $C_{\mathbb{B}}$, or f_{c_2} or f_{c_3} in $C_{\mathbb{B}}$. Thus, a candidate output $y : 2$ corresponds to holding $((x < 10) \wedge \neg(y > 9) \wedge \neg(y \leq x))$ which is exactly f_{c_3} allowed by e_0^+ , but not by e_0 (considered by $\varphi_{\mathbb{B}}$ but not by $\varphi'_{\mathbb{B}}$). Therefore, the corresponding $S_{\mathcal{T}}$ using the winning region W for $\varphi'_{\mathbb{B}}$ would override the output candidate $y : 2$ provided by D (generating an output $v_{\bar{y}}$ such that $v_{\bar{y}}$ holds f_{c_2} ; e.g., $y' : -1$); i.e., it incorrectly interprets that candidate $v_{\bar{y}}$ is dangerous, whereas $S_{\mathcal{T}}$ using the winning region W for $\varphi_{\mathbb{B}}$ would not override $v_{\bar{y}}$.*

The most permissive shield uses the WR of the complete set of valid reactions VR , but note that computing WR and VR is more expensive than $C_{\mathbb{B}}$ and MVR . However, for efficiency reasons the most permissive shield is usually not computed, either because (1) the abstraction algorithm for computing valid reactions computes a non-strict covering or because (2) the synthesis of WR does not terminate (specially in liveness specifications). Note that not only the cost of constructing $S_{\mathcal{T}}$ is relevant, but also other design decisions: if we want the policy of D to dominate, then we need $S_{\mathcal{T}}$ to be as permissive as possible, whereas if we want $\varphi_{\mathcal{T}}$ to dominate (e.g., in specially critical tasks), then we want $S_{\mathcal{T}}$ to be intrusive. Moreover, we can guarantee maximal permissivity computing VR (and WR), whereas we can also guarantee maximal intrusion computing MVR (and $C_{\mathbb{B}}$). Indeed, it is always possible to compute such MVR .

Theorem 4. *Maximally intrusive shield synthesis (i.e., MVR and $C_{\mathbb{B}}$) is decidable.*

Proof. Let R be a feasible set of reactions. Recall that for every $r \in R$, any $r' \neq r$ s.t. $r' \in R$ it holds that either $r \subseteq r'$ or $r' \subseteq r$ or r and r' are not comparable. Thus, for any arbitrary (r, r') where $r, r' \in R$, and r and r' are comparable, we can generate a feasible set R' where either $r \notin R'$ or $r' \notin R'$; in other words, an exhaustive algorithm can remove all the comparable reactions until the fix-point where all of them are not comparable and the resulting R^k is feasible (where k is the number of iterations). Moreover, R'' is exactly MVR . Also, since synthesis of $C_{\mathbb{B}}$ is decidable, then computing the most intrusive $S_{\mathcal{T}}$ is decidable. \square

In Ex. 3 the alternative $\varphi'_{\mathbb{B}}$ that ignores the (playable) choice e_0^+ is exactly comparing $r_{e_0} = \{c_1, c_2\}$ and $r_{e_0^+} = \{c_1, c_2, c_3\}$ and constructing a feasible R' , where $r_{e_0^+} \notin R'$, since $r_{e_0} \subset r_{e_0^+}$. In this case, the fix point is found in only one step and R' is an MVR . There are algorithms (Alg. 1 in (Rodriguez and Sánchez 2023)) that provide a VR set, while others (Alg. 2 and Alg. 3 in (Rodriguez and Sánchez 2023)) produce feasible reaction sets, which are not necessarily MVR . Our proof of Thm. 4 suggests such (exhaustive) algorithm to provide MVR .

3.3 Further Advantages of Shields in \mathcal{T}

Shields Optimized in \mathcal{T} . In Subsec. 3.1 we observed that, given $v_{\bar{x}}$, the **provider** component computes an output $v'_{\bar{y}}$ from c and r such that $v'_{\bar{y}}$ is a model of the formula $\psi = \exists \bar{y}'. (f_r(\bar{x}) \rightarrow f_c(\bar{y}', \bar{x}))[\bar{x} \leftarrow v_{\bar{x}}]$. Moreover, not only is ψ guaranteed to be satisfiable (by Lemma. 1), but usually has several models. This implies that the engineer can select some $v'_{\bar{y}}$ that are preferable over others, depending on different criteria represented by objective functions. Optimization Modulo Theories (OMT) is an extension of SMT that allows model selection based on a given set of constraints (Sebastiani and Trentin 2017). We first describe $S_{\mathcal{T}}$ with linear optimization, which is suitable for arithmetic theories.

Example 4. Recall from Ex. 3 that $x : 0$. Also, for simplicity we consider $f_r = \top$ and $\psi = \exists y'. f_r(x) \rightarrow f_c(x, y')[x \leftarrow 0]$, where $f_c = ((x < 10) \wedge \neg(y' > 9) \wedge \neg(y' \leq x))$. Then, a possible model for ψ is $y' : 2$. However, any value $y' \in [1, 9]$ would a valid choice. Therefore, we can augment ψ with objective functions that explore the range $[1, 9]$ while maximizing different criteria, which we will denote with ψ_{f^+} , for some objective function f^+ . For instance, the engineer might be interested in obtaining the greatest y' possible in ψ , in which case using $f^+ = \max(y')$ would result in ψ_{f^+} —returning $y' : 9$. Additionally, we can optimize linear combinations, e.g., $f^+ = \min(x + y')$ in ψ_{f^+} , which returns $y' : 1$.

Minimizing distances. Although $S_{\mathcal{T}}$ with linear optimization allows enriching $S_{\mathcal{T}}$ with better responses, it suffers from a crucial limitation: it cannot solve ψ_{f^+} , where $f^+ = \min(|y - y'|)$, i.e., the objective function that minimizes the distance between v_y by D and v'_y by $S'_{\mathcal{T}}$. This is because these are not linear properties. However, this optimization would be very relevant in the context of shielding, because, without loss of generality, it expresses that $v'_{\bar{y}}$ is the safe correction by $S_{\mathcal{T}}$ closest to the unsafe $v_{\bar{y}}$ by D . To solve this, we used maximum satisfiability (MaxSMT), which adds soft constraints $\mathcal{M} = \{\phi_1, \phi_2, \dots\}$ to ψ , such that $\psi(\mathcal{M}) = \exists \bar{y}'. (f_c(\bar{x}, \bar{y}') \wedge \bigwedge_{i=1}^{|\mathcal{M}|} \phi_i)[\bar{x} \leftarrow v_{\bar{x}}]$, where \wedge^+ denotes a soft conjunction, meaning that the right-hand side is satisfied only if possible. To better illustrate this, we use a single variable y , although this concept can also be extended to other notions of distance with multiple variables \bar{y} (e.g., Euclidean distance).

Example 5. Consider again Ex. 3 and let $\mathcal{M} = \{(y' > 5)\}$. Then $\psi(\mathcal{M}) = \exists y'. (f_c(x, y') \wedge (y' > 5))[x \leftarrow 0]$ does not return $y' : 2$, but some $y' \in [6, 9]$. In addition, as stated, we can leverage MaxSMT to express that v'_y is the safe correction that is the closest to an unsafe v_y , for which we add $\phi(\bar{x}, y, y') = \forall z. (f_c(\bar{x}, z) \rightarrow (|y' - y| < |z - y|))$ to \mathcal{M} in $\psi(\mathcal{M})$, so that $\psi(\mathcal{M}) = (f_c(\bar{x}, y) \wedge (y' > 5) \wedge \phi(\bar{x}, y, y'))[\bar{x} \leftarrow v_{\bar{x}}, y \leftarrow v_y]$. Thus, given a $y : 4$ labelled as unsafe, $\psi(\mathcal{M})$ will not return an arbitrary model $y' \in [6, 9]$, but the concrete $y' : 6$. This converges in $\mathcal{T}_{\mathbb{Z}}$.

Lemma 4 (Closest element). In $\mathcal{T}_{\mathbb{Z}}$ the following holds. Assuming $\forall \bar{x}. \exists y. f_c(\bar{x}, y)$, the following is also valid:

$$\forall \bar{x}. z. \exists y. (f_c(\bar{x}, y) \wedge \forall w. [f_c(\bar{x}, w) \rightarrow |y - z| \leq |w - z|]).$$

In other words, in $\mathcal{T}_{\mathbb{Z}}$ if for all inputs \bar{x} there is an output y such that ψ holds, then there is always a closest value to any provided z that satisfies ψ . However, for the theory of real arithmetic $\mathcal{T}_{\mathbb{R}}$ it may not be possible to find a value that satisfies $f_c(\bar{x}, y')$ and is the closest to v_y . Instead, it is always possible to compute a closest value within a given tolerance constant ϵ via the addition of the following, soft constraint: $\forall z. (f_c(\bar{x}, z) \rightarrow (|y' - y| < |z - y| + \epsilon))$.

Lemma 5 (Approximately Closest Element). In $\mathcal{T}_{\mathbb{R}}$ the following holds. Assuming $\forall \bar{x}. \exists y. f_c(\bar{x}, y)$, then for every constant $\epsilon > 0$, the following is valid:

$$\forall \bar{x}. z. \exists y. (f_c(\bar{x}, y) \wedge \forall w. [f_c(\bar{x}, w) \rightarrow |y - z| \leq |w - z| + \epsilon]).$$

Note that to enforce $v'_{\bar{y}}$ closest to $v_{\bar{y}}$, we need to additionally extended the **provider** component with input $v_{\bar{y}}$. Also, note that two soft constraints can be contrary to each other, in which case the engineer has to establish priorities using weights. It is also important to note that using soft constraints does not compromise correctness, as any solution found by the solver that supports soft constraints will satisfy the hard constraints as well. Hence, the correctness of Thm. 1 and Thm. 2 remains in-place. Note that not only $S_{\mathcal{T}}$ can minimize the distance to D in arithmetic \mathcal{T} , but in any \mathcal{T} for which engineers define a metric space.

Permissive Optimization. We showed that a $S_{\mathcal{T}}$ can provide an output $v'_{\bar{y}}$ that is the safe correction by closest to the unsafe $v_{\bar{y}}$ by D . Moreover, previously we showed that we can generate multiple strategies using WR . Therefore, we can optimize $v'_{\bar{y}}$ using combinations in the WR ; for instance, return $v'_{\bar{y}}$ such that distance to $v_{\bar{y}}$ is minimal and $v'_{\bar{y}}$ has been chosen among the strategies represented by automata with less than n states (i.e., using bounded synthesis with bound n). We illustrate this using our running example.

Example 6. Consider again $\varphi_{\mathbb{B}}$ and $\varphi'_{\mathbb{B}}$ from Ex. 3 and environment input $x : 0$. For the sake of the argument, consider that the correct output has to satisfy either f_{c_2} (both in e_0 and e_0^+), or f_{c_2} or f_{c_3} (where f_{c_3} appears only in e_0^+). Let the candidate output $y : 11$, which does not correspond to neither f_{c_2} or f_{c_3} , which means that has to be overridden. Now, we want to produce a correction $v'_{\bar{y}}$ as close as possible to $v_{\bar{y}}$. If we only consider e_0 , the best $v'_{\bar{y}}$ (in the distance sense) that we can produce is $y' : 0$, because f_{c_2} has to hold constraint ($y \leq x$). On the contrary, if we consider e_0 , then the best $v'_{\bar{y}}$ we can produce is $y' : 9$ (a higher output is not possible because of constraint ($y \leq 9$) of f_{c_3}).

Theorem 5. Let $\mathcal{T} = \mathcal{T}_{\mathbb{Z}}$ and let a candidate output $v_{\bar{y}}$ considered unsafe. Let a WR in an arbitrary state q_k and an input $v_{\bar{x}}$, which yields a set $C = \{c_k, c_j, c_i, \dots\}$ of choices that are safe for the system. We denote with $F = \{f_{c_k}, f_{c_j}, f_{c_i}\}$ the set of characteristic choice functions. There is always a value v'_y of y' satisfying $f_r(v_{\bar{x}}) \rightarrow f_c(y', v_{\bar{x}})$, where $f_c \in F$, such that for v''_y of y'' satisfying $f_r(v_{\bar{x}}) \rightarrow f'_c(y'', v_{\bar{x}})$, where $f'_c \in F$ and $f_c \neq f'_c$, then the distance from v'_y to $v_{\bar{y}}$ is smaller or equal than the distance from v''_y to $v_{\bar{y}}$.

Note that Thm. 5 holds for other decidable \mathcal{T} . This advantage is unique to $S_{\mathcal{T}}$ and it offers yet another permissivity layer to measure distance with respect to the policy of D .

4 Evaluation and Practical Implications

4.1 Completeness in Fully Observable Domains

Case Study: GridWorld. We demonstrate that in scenarios that are *fully observable*, $S_{\mathcal{T}}$ can be *complete* in the sense that it is possible to fully guarantee safety. Gridworld (GW) is a standard DRL benchmark (Bassan et al. 2023), in which an agent navigates on a two-dimensional grid (see leftmost side of Fig. 2) and its goal is to reach a target destination while adhering to some additional requirements. Typically, GW has a discrete state space representing the coordinates of the cells. However, to show the capabilities of our shielding approach, we modify the scenario to obtain a continuous state space by adding Gaussian noise to the agent’s position, resulting in inputs in the domain of $\mathcal{T}_{\mathbb{R}}$. We note that this also makes the problem *significantly* harder. One main advantage of GW is that it is a *fully observable* system, i.e., we can manually encode a complete set of requirements that, if respected, guarantee that $D \cdot S_{\mathcal{T}}$ never violates a *high-level* behaviour, e.g., *never collide*. In other words, $S_{\mathcal{T}}$ can only enforce $D \cdot S_{\mathcal{T}}$ based on $\varphi_{\mathcal{T}}$, whereas successfully avoiding collisions depends on whether the properties captured by $\varphi_{\mathcal{T}}$ cover all possible traces. This is possible in GW and other fully observable systems. We chose the natural safety specification — *do not collide at the next time-step*, and we demonstrate how our shield can guarantee that this specification is never violated.



Figure 2: GridWorld, left to right: A scheme of the benchmark arena, and the average success rate and collision rate obtained during the DRL training process.

Results. We trained a pool of 500 models, differing in the random seed used to generate them. Next, we retained only the models that demonstrated very high performance, i.e., reached our cutoff threshold of a 98% success rate, with successful trajectories in over 100 consecutive trials (see center images in Fig. 2). We also point out that even after extensive training, there was not a single model that achieved a 0% collision rate (see rightmost image in Fig. 2). We note that this is in line with previous research on DRL safety, which demonstrated that even state-of-the-art agents may indeed violate simple safety requirements (Amir et al. 2023a; Amir, Schapira, and Katz 2021; Kazak et al. 2019) — further motivating the need for shielding even in this, relatively simple, task. Next, we showcase that $S_{\mathcal{T}}$ can efficiently eliminate collisions via the usage of safety properties that cause the agent to collide in the next time-step, and overriding these, unwanted actions. For example, if the agent is near an obstacle on the left ³ then it should not select the

³Represented with the continuous input $\bar{x} = \{x_0, x_1, \dots, x_7\}$,

next action to be LEFT. We now analyze the runtime impact of $S_{\mathcal{T}}$ on real executions of $D \cdot S_{\mathcal{T}}$. Tab. 1 present the first 10 results, where we can see that our proposed solution successfully eliminates all possible collisions, resulting in safer behavior. Nevertheless, we point out that the increased safety did not compromise the general performance of the agent, as can be seen by the unaltered success rate.

Seed	Without Shield		With Shield		Overhead
	Succ.	Coll.	Succ.	Coll.	
0	89%	3%	89%	0%	219.1%
1	92%	1%	93%	0%	182.4%
2	91%	2%	92%	0%	204.6%
3	91%	3%	91%	0%	240.9%
4	92%	2%	92%	0%	206.5%
5	89%	1%	90%	0%	213.1%
6	92%	2%	92%	0%	212.1%
7	86%	6%	91%	0%	250.9%
8	92%	1%	92%	0%	226.2%
9	89%	3%	91%	0%	220.0%

Table 1: A performance comparison for the agent with and without the safety shield. The values are obtained over 100 episodes for each of the seeds.

Although $D \cdot S_{\mathcal{T}}$ completely avoids collisions, this comes at a price: $D \cdot S_{\mathcal{T}}$ checks in each time-step whether $(v_{\bar{x}}, v_{\bar{y}})$ is correct with respect to $\varphi_{\mathcal{T}}$ (and overrides it if not). This, in turn, introduces a computational overhead in the execution. In the case of GW, we note that the overhead is significant (around 200%), which suggests that the choice of using a more permissive $S_{\mathcal{T}}$ (see Subsec. 3.2), might be preferable in domains where runtime optimization is essential. Note that success ratios do not necessarily increase to 100% when shielded, as collision avoidance may cause some loops instead of collisions. Nevertheless success never decreases.

4.2 Temporal Dynamics

We now show how $S_{\mathcal{T}}$ can manage both rich data and temporal dynamics. To do so, we used 13 different specifications from (Wu et al. 2019), which are, to the best of our knowledge, the only previous successful attempt to compute rich-data shields. We generated our shield and measured time for computing: (i) the Boolean step (columns \mathbb{B}), and (ii) producing the final output (columns \mathcal{T}). We compared our results at Tab. 2. For the first task, our approach, on average, requires less than 0.21 μ s, while (Wu et al. 2019) takes more than twice as long on average (with over 0.47 μ s). Our approach was also more efficient in the second task, taking on average about 0.157ms, whereas (Wu et al. 2019) required 0.557ms on average. Moreover, note that our (\mathbb{B}) contains both detection and correction of candidate outputs, whereas (\mathbb{B}) of (Wu et al. 2019) only contains detection.

It is important to note another key advantage of our approach: (Wu et al. 2019) necessarily generates a WR , whereas we can also construct $C_{\mathcal{T}}$ (column \mathbb{B}'), performs considerably faster (and can operate leveraging highly matured techniques, e.g., bounded synthesis). In addition to

where $x_0 \in [0.05, 0.15]$, $x_1 \in [0.05, 0.15]$, ..., $x_7 \in [0.05, 0.15]$.

Req.	(Wu et al.)		Ours					
	\mathbb{B}	\mathcal{T}	\mathbb{B}	\mathbb{B}'	\mathcal{T}	$\mathcal{T}_{\mathbb{Z}}$	\mathcal{T}_A	\mathcal{T}_B
φ_0	.30	631	.19	.17	171	173	183	184
φ_1	.41	590	.22	.21	190	192	199	212
φ_2	.80	520	.24	.20	214	194	214	199
φ_3	.45	340	.22	.18	106	105	120	105
φ_4	.50	640	.21	.17	118	122	120	117
φ_5	.80	520	.21	.16	124	124	127	156
φ_6	.37	370	.16	.14	141	156	148	151
φ_7	.49	710	.20	.20	163	159	165	173
φ_8	.45	580	.21	.15	133	134	143	189
φ_9	.18	610	.14	.11	170	179	172	203
φ_{10}	.50	690	.25	.19	173	168	182	177
φ_{11}	.31	530	.21	.17	177	178	191	177
φ_{12}	.57	510	.29	.22	156	155	179	182

Table 2: Comparison of (Wu et al. 2019) and our approach (in μs)

this, we (Wu et al. 2019) presents a monolithic method that to be used with specifications containing only linear real arithmetic $\mathcal{T}_{\mathbb{Z}}$. Hence, if we slightly modify \mathcal{T} to $\mathcal{T}_{\mathbb{Z}}$, then the method in (Wu et al. 2019) cannot provide an appropriate shield, whereas we do (column $\mathcal{T}_{\mathbb{Z}}$) (neither for non-linear \mathcal{T}). In contrast, our method encodes *any* arbitrary $\exists^*\forall^*$ decidable fragment of \mathcal{T} (e.g., non-linear arithmetic or the array property fragment (Bradley, Manna, and Sipma 2006)). Additionally, we can optimize the outputs of $S_{\mathcal{T}}$ with respect to different criteria, such as returning the smallest/greatest safe output (column \mathcal{T}_A) and the output closest to the candidate (column \mathcal{T}_B), for which we used Z3 with OMT (Björner and A. 2014; Björner, Phan, and Fleckenstein 2015). These experiments show the applicability of our approach.⁴

5 Related Work and Conclusion

Related Work. Classic shielding approaches (Bloem et al. 2015; Könighofer et al. 2017; Alshiekh et al. 2018; Jansen et al. 2018; Avni et al. 2019; Tappler et al. 2022; Córdoba et al. 2023) focus on properties expressed in Boolean LTL, and are incompatible for systems with richer-data domains: i.e., they need explicit **manual** discretization of the requirements. In the other hand, we have a sound procedure that directly takes $LTL_{\mathcal{T}}$ specifications, which is fundamentally new. Other, more recent, work (Rodríguez and Sánchez 2023; Rodríguez and Sánchez 2024a; Rodríguez and Sánchez 2024b) proves that, under certain conditions, $LTL_{\mathcal{T}}$ synthesis is decidable via abstraction methods, which can be understood as computing *minterms* to produce symbolic automata and transducers (D’Antoni and Veanes 2017) from reactive specifications, and using antichain-based optimization, as suggested by (Veanes et al. 2023). We complement and extend these techniques and demonstrate that they can act as a basis for shields synthesis modulo theories, which also contains an error detection phase whose design is essential for permissivity and which can optimize the output with respect to the erroneous candi-

⁴Note that because of space limitations we could not include experiments over real robots in the main text (see suppl. material)

date. Our work also includes an in-depth comparison to (Wu et al. 2019), that present a competing method for synthesizing shields in the \mathcal{T} of linear real arithmetic, which does not cover such an expressive fragment and only computes WR.

As for reactive synthesis, methods for infinite theories have also been proposed. Moreover, some of them consider a expressive temporal logics where not only multi-step properties can be defined, but also variables can convey information across-time (Finkbeiner, Heim, and Passing 2022). However, they do not guarantee success (Katis et al. 2016) or termination (Katis et al. 2016; Katis et al. 2018; Gacek et al. 2015; Choi et al. 2022; Maderbacher and Bloem 2022), and can be unsound for some cases (Gacek et al. 2015) or may need guidance (Walker and Ryzhyk 2014). Therefore, any shield synthesis techniques derived from these would be incomplete. Runtime enforcement (Schneider 2000; Ligatti, Bauer, and Walker 2009; Falcone, Fernandez, and Mounier 2012) is an additional technique similar to shielding, but it is not compatible with reactive systems (Bloem et al. 2015). In addition, supervisory control of discrete event systems (Cassandras and Lafortune 1999) is based on invariant specifications and controllable events, and while reactive shield-synthesis additionally admits rich temporality, supervisory control cannot be applied to temporal settings (e.g., the one presented in Subsec. 4.2).

Other approaches for ensuring DNN safety rely on formal verification (Katz et al. 2017; Katz et al. 2019; Ehlers 2017; Bunel et al. 2018; Tran et al. 2020; Tran, Bak, and Johnson 2020; Ashok et al. 2020; Huang et al. 2017; Zhang et al. 2018; Wang et al. 2021; Corsi, Marchesini, and Farinelli 2021; Lopez et al. 2023; Amir et al. 2021; Amir et al. 2022; Amir et al. 2023b; Amir et al. 2023c; Corsi et al. 2024; Mandal et al. 2024; Bassan and Katz 2023; Casadio et al. 2022; Wu et al. 2024) and Scenario-Based Programming (Corsi et al. 2022; Yerushalmi et al. 2022; Yerushalmi et al. 2023). but they have limited scalability and expressivity.

Conclusion. In this work, we present the first general methods for shielding properties encoded in $LTL_{\mathcal{T}}$. These allows engineers to guarantee the safe behavior of DRL agents in complex, reactive environments. Specifically, we demonstrate how shields can be computed from a controller and from a winning region. This is not simply a direct application of synthesis, instead, we can guarantee maximally and minimally permissive shields, as well as shields optimized with respect to objective functions in arbitrary decidable \mathcal{T} . We also empirically demonstrate its applicability.

A next step is to adapt shields modulo theories to probabilistic settings (e.g., shielding POMDPs) (Pranger et al. 2021a; Pranger et al. 2021b; Carr et al. 2022; Carr et al. 2023). Also, we plan on incorporating our shield along with complementary DNN verification engines. Another direction of future work relies on recent results for satisfiability of finite-trace $LTL_{\mathcal{T}}$ (Geatti et al. 2023), as we aim to identify fragments of $LTL_{\mathcal{T}}$ with across-time data-transfer for which reactive synthesis is decidable. Future work may also include $LTL_{\mathcal{T}}$ shields for multi-agent and planning scenarios (Bharadwaj et al. 2019; Camacho, Bienvenu, and McIl-

raith 2019; Street et al. 2020; Lin and Bercher 2022), and combinations with uncertainty or continuous time (Tiger and Heintz 2020; Street et al. 2022; Yu, Lee, and Bae 2022; Carreno et al. 2022). We want to adapt results to finite traces (Giacomo and Vardi 2013), since our agents either collide, reach the goal or have a time limit (unknown a priori).

Acknowledgments

The work of Rodríguez and Sánchez was funded in part by PRODIGY Project (TED2021-132464B-I00) — funded by MCIN/AEI/10.13039/501100011033/ and the European Union NextGenerationEU/PRTR — by the DECO Project (PID2022-138072OB-I00) — funded by MCIN/AEI/10.13039/501100011033 and by the ESF, as well as by a research grant from Nomadic Labs and the Tezos Foundation. The work of Amir and Katz was partially funded by the European Union (ERC, VeriDeL, 101112713). Views and opinions expressed are however those of the author(s) only and do not necessarily reflect those of the European Union or the European Research Council Executive Agency. Neither the European Union nor the granting authority can be held responsible for them. The work of Amir was further supported by a scholarship from the Clore Israel Foundation.

References

- Alshiekh, M.; Bloem, R.; Ehlers, R.; Könighofer, B.; Niekum, S.; and Topcu, U. 2018. Safe Reinforcement Learning via Shielding. In *Proc. of the 32nd AAAI Conference on Artificial Intelligence*, 2669–2678.
- Amir, G.; Wu, H.; Barrett, C.; and Katz, G. 2021. An SMT-Based Approach for Verifying Binarized Neural Networks. In *Proc. 27th Int. Conf. on Tools and Algorithms for the Construction and Analysis of Systems (TACAS)*, 203–222.
- Amir, G.; Zelazny, T.; Katz, G.; and Schapira, M. 2022. Verification-Aided Deep Ensemble Selection. In *Proc. 22nd Int. Conf. on Formal Methods in Computer-Aided Design (FMCAD)*, 27–37.
- Amir, G.; Corsi, D.; Yerushalmi, R.; Marzari, L.; Harel, D.; Farinelli, A.; and Katz, G. 2023a. Verifying Learning-Based Robotic Navigation Systems. In *Proc. 29th Int. Conf. on Tools and Algorithms for the Construction and Analysis of Systems (TACAS)*, 607–627.
- Amir, G.; Freund, Z.; Katz, G.; Mandelbaum, E.; and Refaeli, I. 2023b. veriFIRE: Verifying an Industrial, Learning-Based Wildfire Detection System. In *Proc. 25th Int. Symposium on Formal Methods (FM)*, 648–656.
- Amir, G.; Maayan, O.; Zelazny, T.; Katz, G.; and Schapira, M. 2023c. Verifying Generalization in Deep Learning. In *Proc. 35th Int. Conf. on Computer Aided Verification (CAV)*, 438–455.
- Amir, G.; Schapira, M.; and Katz, G. 2021. Towards Scalable Verification of Deep Reinforcement Learning. In *Proc. 21st Int. Conf. on Formal Methods in Computer-Aided Design (FMCAD)*, 193–203.
- Ashok, P.; Hashemi, V.; Kretinsky, J.; and Mühlberger, S. 2020. DeepAbstract: Neural Network Abstraction for Accelerating Verification. In *Proc. 18th Int. Symposium on Automated Technology for Verification and Analysis (ATVA)*.
- Avni, G.; Bloem, R.; Chatterjee, K.; Henzinger, T. A.; Könighofer, B.; and Pranger, S. 2019. Run-time optimization for learned controllers through quantitative games. In *Proc. of the 31st International Conference in Computer Aided Verification (CAV), Part I*, volume 11561 of *LNCS*, 630–649. Springer.
- Bassan, S., and Katz, G. 2023. Towards Formal Approximated Minimal Explanations of Neural Networks. In *Proc. 29th Int. Conf. on Tools and Algorithms for the Construction and Analysis of Systems (TACAS)*, 187–207.
- Bassan, S.; Amir, G.; Corsi, D.; Refaeli, I.; and Katz, G. 2023. Formally Explaining Neural Networks within Reactive Systems. In *Proc. 23rd Int. Conf. on Formal Methods in Computer-Aided Design (FMCAD)*, 10–22.
- Bernreiter, M.; Maly, J.; and Woltran, S. 2021. Choice Logics and Their Computational Properties. In *Proc. of the 30th Int. Joint Conf. on Artificial Intelligence, (IJCAI 2021)*, 1794–1800.
- Bharadwaj, S.; Bloem, R.; Dimitrova, R.; Könighofer, B.; and Topcu, U. 2019. Synthesis of minimum-cost shields for multi-agent systems. In *2019 American Control Conference, ACC 2019, Philadelphia, PA, USA, July 10-12, 2019*, 1048–1055. IEEE.
- Bjørner, N., and A., P. 2014. νZ - Maximal Satisfaction with Z3. In *Proc. of the 6th Int. Symposium on Symbolic Computation in Software Science, (SCSS)*, volume 30, 1–9.
- Bjørner, N.; Phan, A.; and Fleckenstein, L. 2015. νZ - An Optimizing SMT Solver. In *Proc. of the 21st Int. Conf. on Tools and Algorithms for the Construction and Analysis of Systems (TACAS)*, volume 9035, 194–199.
- Bloem, R.; Könighofer, B.; Könighofer, R.; and Wang, C. 2015. Shield Synthesis: - Runtime Enforcement for Reactive Systems. In *Proc. of the 21st Int. Conf. in Tools and Algorithms for the Construction and Analysis of Systems, (TACAS)*, volume 9035, 533–548.
- Bradley, A. R., and Manna, Z. 2007. *The calculus of computation - decision procedures with applications to verification*. Springer.
- Bradley, A.; Manna, Z.; and Sipma, H. 2006. What’s Decidable About Arrays? In *Proc. of the 7th Int. Conf. on Verification, Model Checking, and Abstract Interpretation (VMCAI)*, 427–442.
- Brenguier, R.; Pérez, G. A.; Raskin, J.; and Sankur, O. 2014. Absynthe: abstract synthesis from succinct safety specifications. In *Proc. of the 3rd Workshop on Synthesis, (SYNT 2014)*, volume 157 of *EPTCS*, 100–116.
- Bunel, R.; Turkaslan, I.; Torr, P.; Kohli, P.; and Mudigonda, P. 2018. A Unified View of Piecewise Linear Neural Network Verification. In *Proc. 32nd Conf. on Neural Information Processing Systems (NeurIPS)*, 4795–4804.
- Camacho, A.; Bienvenu, M.; and McIlraith, S. A. 2019. Towards a unified view of AI planning and reactive synthesis. In *Proc. of the 29th International Conference on*

- Automated Planning and Scheduling (ICAPS 2019)*, 58–67. AAAI Press.
- Carr, S.; Jansen, N.; Junges, S.; and Topcu, U. 2022. Safe reinforcement learning via shielding for pomdps. *CoRR* abs/2204.00755.
- Carr, S.; Jansen, N.; Junges, S.; and Topcu, U. 2023. Safe reinforcement learning via shielding under partial observability. In *Proc. of the 37th Conference on Artificial Intelligence (AAAI 2023)*, 14748–14756. AAAI Press.
- Carreno, Y.; Ng, J. H. A.; Petillot, Y. R.; and Petrick, R. P. A. 2022. Planning, execution, and adaptation for multi-robot systems using probabilistic and temporal planning. In *Proc. of the 21st International Conference on Autonomous Agents and Multiagent (AAMAS 2022)*, 217–225. International Foundation for Autonomous Agents and Multiagent Systems (IFAAMAS).
- Casadio, M.; Komendantskaya, E.; Daggitt, M.; Kokke, W.; Katz, G.; Amir, G.; and Refaeli, I. 2022. Neural Network Robustness as a Verification Property: A Principled Case Study. In *Proc. 34th Int. Conf. on Computer Aided Verification (CAV)*, 219–231.
- Cassandras, C. G., and Lafortune, S. 1999. *Introduction to Discrete Event Systems*, volume 11 of *The Kluwer International Series on Discrete Event Dynamic Systems*. Springer.
- Choi, W.; Finkbeiner, B.; Piskac, R.; and Santolucito, M. 2022. Can Reactive Synthesis and Syntax-Guided Synthesis be Friends? In *Proc. of the 43rd ACM SIGPLAN Int. Conf. on Programming Language Design and Implementation (PLDI)*, 229–243.
- Córdoba, F. C.; Palmisano, A.; Fränzle, M.; Bloem, R.; and Könighofer, B. 2023. Safety shielding under delayed observation. In *Proc. of the 33th International Conference on Automated Planning and Scheduling (ICAPS’23)*, 80–85. AAAI Press.
- Corsi, D.; Yerushalmi, R.; Amir, G.; Farinelli, A.; Harel, D.; and Katz, G. 2022. Constrained Reinforcement Learning for Robotics via Scenario-Based Programming. Technical Report. <https://arxiv.org/abs/2206.09603>.
- Corsi, D.; Amir, G.; Katz, G.; and Farinelli, A. 2024. Analyzing Adversarial Inputs in Deep Reinforcement Learning. Technical Report. <https://arxiv.org/abs/2402.05284>.
- Corsi, D.; Marchesini, E.; and Farinelli, A. 2021. Formal verification of neural networks for safety-critical tasks in deep reinforcement learning. In *Uncertainty in Artificial Intelligence*.
- D’Antoni, L., and Veanes, M. 2017. The power of symbolic automata and transducers. In *Proc. of the 29th International Conference in Computer Aided Verification (CAV 2017)*, Part I, volume 10426 of *LNCS*, 47–67. Springer.
- de Moura, L. M., and Bjørner, N. S. 2008. Z3: an efficient SMT solver. In *Proc. of the 14th International Conference on Tools and Algorithms for the Construction and Analysis of Systems, 14th International Conference, (TACAS 2008)*, volume 4963 of *LNCS*, 337–340. Springer.
- Ehlers, R. 2017. Formal Verification of Piece-Wise Linear Feed-Forward Neural Networks. In *Proc. 15th Int. Symp. on Automated Technology for Verification and Analysis (ATVA)*, 269–286.
- Falcone, Y.; Fernandez, J.; and Mounier, L. 2012. What can you Verify and Enforce at Runtime? *Int. J. Softw. Tools Technol. Transf.* 14(3):349–382.
- Fedyukovich, G.; Gurfinkel, A.; and Gupta, A. 2019. Lazy but effective functional synthesis. In *Proc. of the 20th International Conference in Verification on Model Checking, and Abstract Interpretation, (VMCAI 2019)*, volume 11388 of *LNCS*, 92–113. Springer.
- Finkbeiner, B.; Heim, P.; and Passing, N. 2022. Temporal Stream Logic Modulo Theories. In *Proc of the 25th Int. Conf. on Foundations of Software Science and Computation Structures, (FOSSACS 2022)*, volume 13242 of *LNCS*, 325–346.
- Fontaine, P. 2007. Combinations of theories and the bernays-schönfinkel-ramsey class. In *Proceedings of 4th International Verification Workshop in connection with CADE-21 (VERIFY 2007)*, volume 259 of *CEUR Workshop Proceedings*. CEUR-WS.org.
- Gacek, A.; Katis, A.; Whalen, M. W.; Backes, J.; and Cofer, D. D. 2015. Towards realizability checking of contracts using theories. In *Proc. of the 7th International Symposium NASA Formal Methods (NFM 2015)*, volume 9058 of *LNCS*, 173–187. Springer.
- Geatti, L.; Gianola, A.; Gigante, N.; and Winkler, S. 2023. Decidable fragments of ltlf modulo theories (extended version). *CoRR* abs/2307.16840.
- Gehr, T.; Mirman, M.; Drachler-Cohen, D.; Tsankov, E.; Chaudhuri, S.; and Vechev, M. 2018. AI2: Safety and Robustness Certification of Neural Networks with Abstract Interpretation. In *Proc. 39th IEEE Symposium on Security and Privacy (S&P)*.
- Giacomo, G. D., and Vardi, M. Y. 2013. Linear temporal logic and linear dynamic logic on finite traces. In *Proc. of the 23rd Int’l Joint Conference on Artificial Intelligence (IJCAI 2013,)*, 854–860. IJCAI/AAAI.
- Goodfellow, I.; Bengio, Y.; and Courville, A. 2016. *Deep Learning*. MIT Press.
- Goodfellow, I.; Shlens, J.; and Szegedy, C. 2014. Explaining and Harnessing Adversarial Examples. Technical Report. <http://arxiv.org/abs/1412.6572>.
- Huang, X.; Kwiatkowska, M.; Wang, S.; and Wu, M. 2017. Safety Verification of Deep Neural Networks. In *Proc. 29th Int. Conf. on Computer Aided Verification (CAV)*, 3–29.
- Jansen, N.; Könighofer, B.; Junges, S.; and Bloem, R. 2018. Shielded decision-making in mdps. *CoRR* abs/1807.06096.
- Katis, A.; Fedyukovich, G.; Gacek, A.; Backes, J. D.; Gurfinkel, A.; and Whalen, M. W. 2016. Synthesis from assume-guarantee contracts using skolemized proofs of realizability. *CoRR* abs/1610.05867.
- Katis, A.; Fedyukovich, G.; Guo, H.; Gacek, A.; Backes, J.; Gurfinkel, A.; and Whalen, M. W. 2018. Validity-guided synthesis of reactive systems from assume-guarantee contracts. In *Proc. of the 24th International Conference on Tools and Algorithms for the Construction and Analysis of*

- Systems, (TACAS 2018)*, volume 10806 of *LNCS*, 176–193. Springer.
- Katz, G.; Barrett, C.; Dill, D.; Julian, K.; and Kochenderfer, M. 2017. Reluplex: An Efficient SMT Solver for Verifying Deep Neural Networks. In *Proc. 29th Int. Conf. on Computer Aided Verification (CAV)*, 97–117.
- Katz, G.; Huang, D.; Ibeling, D.; Julian, K.; Lazarus, C.; Lim, R.; Shah, P.; Thakoor, S.; Wu, H.; Zeljić, A.; Dill, D.; Kochenderfer, M.; and Barrett, C. 2019. The Marabou Framework for Verification and Analysis of Deep Neural Networks. In *Proc. 31st Int. Conf. on Computer Aided Verification (CAV)*, 443–452.
- Kazak, Y.; Barrett, C.; Katz, G.; and Schapira, M. 2019. Verifying Deep-RL-Driven Systems. In *Proc. 1st ACM SIGCOMM Workshop on Network Meets AI & ML (NetAI)*, 83–89.
- Könighofer, B.; Alshiekh, M.; Bloem, R.; Humphrey, L. R.; Könighofer, R.; Topcu, U.; and Wang, C. 2017. Shield synthesis. *Formal Methods Syst. Des.* 51(2):332–361.
- Li, Y. 2017. Deep Reinforcement Learning: An Overview. Technical Report. <http://arxiv.org/abs/1701.07274>.
- Ligatti, J.; Bauer, L.; and Walker, D. 2009. Run-time enforcement of nonsafety policies. *ACM Trans. Inf. Syst. Secur.* 12(3):19:1–19:41.
- Lin, S., and Bercher, P. 2022. On the expressive power of planning formalisms in conjunction with LTL. In *Proc. of the 32nd International Conference on Automated Planning and Scheduling (ICAPS 2022)*, 231–240. AAAI Press.
- Lopez, D. M.; Choi, S. W.; Tran, H.; and Johnson, T. T. 2023. NNV 2.0: The neural network verification tool. In *Proc. of the 35th International Conference in Computer Aided Verification (CAV 2023), Part II*, volume 13965 of *LNCS*, 397–412. Springer.
- Lyu, Z.; Ko, C. Y.; Kong, Z.; Wong, N.; Lin, D.; and Daniel, L. 2020. Fastened Crown: Tightened Neural Network Robustness Certificates. In *Proc. 34th AAAI Conf. on Artificial Intelligence (AAAI)*, 5037–5044.
- Maderbacher, B., and Bloem, R. 2022. Reactive synthesis modulo theories using abstraction refinement. In *Proc. of the 22nd Conference on Formal Methods in Computer-Aided Design, (FMCAD 2022)*, 315–324. IEEE.
- Mandal, U.; Amir, G.; Wu, H.; Daukantas, I.; Newell, F.; Ravaoli, U.; Meng, B.; Durling, M.; Ganai, M.; Shim, T.; Katz, G.; and Barrett, C. 2024. Formally Verifying Deep Reinforcement Learning Controllers with Lyapunov Barrier Certificates. Technical Report. <https://arxiv.org/abs/2405.14058>.
- Manna, Z., and Pnueli, A. 1995. *Temporal Verification of Reactive Systems: Safety*. Springer Science & Business Media.
- Marchesini, E., and Farinelli, A. 2020. Discrete deep reinforcement learning for mapless navigation. In *2020 IEEE International Conference on Robotics and Automation (ICRA)*.
- Marchesini, E.; Corsi, D.; and Farinelli, A. 2021a. Benchmarking Safe Deep Reinforcement Learning in Aquatic Navigation. In *Proc. IEEE/RSJ Int. Conf on Intelligent Robots and Systems (IROS)*.
- Marchesini, E.; Corsi, D.; and Farinelli, A. 2021b. Exploring Safer Behaviors for Deep Reinforcement Learning. In *Proc. 35th AAAI Conf. on Artificial Intelligence (AAAI)*.
- Marzari, L.; Corsi, D.; Cicalese, F.; and Farinelli, A. 2023. The #dnn-verification problem: Counting unsafe inputs for deep neural networks. *arXiv preprint arXiv:2301.07068*.
- Meyer, P.; Sickert, S.; and Luttenberger, M. 2018. Strix: Explicit Reactive Synthesis Strikes Back! In *Proc. of the 30th Int. Conf. on Computer Aided Verification (CAV)*, 578–586.
- Nandkumar, C.; Shukla, P.; and Varma, V. 2021. Simulation of Indoor Localization and Navigation of Turtlebot 3 using Real Time Object Detection. In *Proc. Int. Conf. on Disruptive Technologies for Multi-Disciplinary Research and Applications (CENTCON)*.
- Optimization, G. 2021. The Gurobi MILP Solver. <https://www.gurobi.com/>.
- Piterman, N.; Pnueli, A.; and Sa’ar, Y. 2006. Synthesis of Reactive (1) Designs. In *Proc. 7th Int. Conf. on Verification, Model Checking, and Abstract Interpretation (VMCAI)*, 364–380.
- Pnueli, A. 1977. The Temporal Logic of Programs. In *Proc. of 18th Annual Symposium on Foundations of Computer Science (SFCS)*, 46–57.
- Pore, A.; Corsi, D.; Marchesini, E.; Dall’Alba, D.; Casals, A.; Farinelli, A.; and Fiorini, P. 2021. Safe Reinforcement Learning using Formal Verification for Tissue Retraction in Autonomous Robotic-Assisted Surgery. In *Proc. IEEE/RSJ Int. Conf. on Intelligent Robots and Systems (IROS)*, 4025–4031.
- Pranger, S.; Könighofer, B.; Posch, L.; and Bloem, R. 2021a. TEMPEST - Synthesis Tool for Reactive Systems and Shields in Probabilistic Environments. In *Proc. 19th Int. Symposium in Automated Technology for Verification and Analysis, (ATVA)*, volume 12971, 222–228.
- Pranger, S.; Könighofer, B.; Tappler, M.; Deixelberger, M.; Jansen, N.; and Bloem, R. 2021b. Adaptive Shielding under Uncertainty. In *American Control Conference, (ACC)*, 3467–3474.
- Reynolds, A.; Iosif, R.; and Serban, C. 2017. Reasoning in the bernays-schönfinkel-ramsey fragment of separation logic. In *18th International Conference on Verification, Model Checking, and Abstract Interpretation (VMCAI 2017)*, volume 10145 of *LNCS*, 462–482. Springer.
- Rodriguez, A., and Sánchez, C. 2023. Boolean abstractions for realizability modulo theories. In *Proc. of the 35th International Conference on Computer Aided Verification (CAV’23)*, volume 13966 of *LNCS*. Springer, Cham.
- Rodriguez, A., and Sánchez, C. 2024a. Realizability modulo theories. *Journal of Logical and Algebraic Methods in Programming* 100971.
- Rodriguez, A., and Sánchez, C. 2024b. Adaptive Reactive Synthesis for LTL and LTLf Modulo Theories. In *Proc. of the 38th AAAI Conf. on Artificial Intelligence (AAAI 2024)*.

- Rodríguez, A., and Sanchez, C. 2023. From Realizability Modulo Theories to Synthesis Modulo Theories Part 1: Dynamic approach. 2310.07904.
- Ruan, X.; Ren, D.; Zhu, X.; and Huang, J. 2019. Mobile Robot Navigation Based on Deep Reinforcement Learning. In *2019 Chinese control and decision conference (CCDC)*.
- Schewe, S., and Finkbeiner, B. 2007. Bounded synthesis. In *Proc. of the 5th International Symposium in Automated Technology for Verification and Analysis (ATVA 2007)*, volume 4762 of *LNCS*, 474–488. Springer.
- Schneider, F. B. 2000. Enforceable security policies. *ACM Trans. Inf. Syst. Secur.* 3(1):30–50.
- Schulman, J.; Wolski, F.; Dhariwal, P.; Radford, A.; and Klimov, O. 2017. Proximal Policy Optimization Algorithms. Technical Report. <http://arxiv.org/abs/1707.06347>.
- Sebastiani, R., and Trentin, P. 2017. On optimization modulo theories, maxsmt and sorting networks. In *Tools and Algorithms for the Construction and Analysis of Systems - Proc. of the 23rd International Conference, (TACAS 2017)*, volume 10206 of *LNCS*, 231–248.
- Street, C.; Lacerda, B.; Mühligh, M.; and Hawes, N. 2020. Multi-robot planning under uncertainty with congestion-aware models. In *Proc. of the 19th International Conference on Autonomous Agents and Multiagent Systems (AAMAS '20)*, 1314–1322. International Foundation for Autonomous Agents and Multiagent Systems.
- Street, C.; Lacerda, B.; Staniaszek, M.; Mühligh, M.; and Hawes, N. 2022. Context-aware modelling for multi-robot systems under uncertainty. In *Proc. of the 21st International Conference on Autonomous Agents and Multiagent Systems (AAMAS 2022)*, 1228–1236. International Foundation for Autonomous Agents and Multiagent Systems (IFAAMAS).
- Sutton, R., and Barto, A. 2018. *Reinforcement Learning: An Introduction*. MIT press.
- Tappler, M.; Pranger, S.; Könighofer, B.; Muskardin, E.; Bloem, R.; and Larsen, K. G. 2022. Automata learning meets shielding. In *Proc. of the 11th International Symposium in Leveraging Applications of Formal Methods, Verification and Validation. Verification Principles (IsoLA 2022), Part I*, volume 13701 of *Lecture Notes in Computer Science*, 335–359. Springer.
- Thomas, W. 2008. Church’s Problem and a Tour Through Automata Theory. In *Pillars of Computer Science*. Springer. 635–655.
- Tiger, M., and Heintz, F. 2020. Incremental reasoning in probabilistic signal temporal logic. *Int. J. Approx. Reason.* 119:325–352.
- Tran, H.; Bak, S.; and Johnson, T. 2020. Verification of Deep Convolutional Neural Networks Using ImageStars. In *Proc. 32nd Int. Conf. on Computer Aided Verification (CAV’22)*, 18–42.
- Tran, H.; Yang, X.; Lopez, D. M.; Musau, P.; Nguyen, L. V.; Xiang, W.; Bak, S.; and Johnson, T. T. 2020. NNV: the neural network verification cyber tool for deep neural networks and learning-enabled cyber-physical systems. In *Proc. of the 32nd International Conference in Computer Aided Verification (CAV’20), Part I*, volume 12224 of *Lecture Notes in Computer Science*, 3–17. Springer.
- Van Hasselt, H.; Guez, A.; and Silver, D. 2016. Deep Reinforcement Learning with Double Q-Learning. In *Proc. 30th AAAI Conf. on Artificial Intelligence (AAAI)*.
- Veanes, M.; Ball, T.; Ebner, G.; and Saarikivi, O. 2023. Symbolic automata: ω -regularity modulo theories. *CoRR* abs/2310.02393.
- Walker, A., and Ryzhyk, L. 2014. Predicate abstraction for reactive synthesis. In *Proc. of the 14th Formal Methods in Computer-Aided Design, (FMCAD 2014)*, 219–226. IEEE.
- Wang, S.; Pei, K.; Whitehouse, J.; Yang, J.; and Jana, S. 2018. Formal Security Analysis of Neural Networks using Symbolic Intervals. In *Proc. 27th USENIX Security Symposium*, 1599–1614.
- Wang, S.; Zhang, H.; Xu, K.; Lin, X.; Jana, S.; Hsieh, C.; and Kolter, Z. 2021. Beta-Crown: Efficient Bound Propagation with per-Neuron Split Constraints for Neural Network Robustness Verification. In *Proc. 34th Conf. on Neural Information Processing Systems (NeurIPS)*, volume 34, 29909–29921.
- Wu, M.; Wang, J.; Deshmukh, J.; and Wang, C. 2019. Shield synthesis for real: Enforcing safety in cyber-physical systems. In *Proc. of 19th Formal Methods in Computer Aided Design, (FMCAD 2019), San Jose, CA, USA, October 22-25, 2019*, 129–137. IEEE.
- Wu, H.; Isac, O.; Zeljić, A.; Tagomori, T.; Daggitt, M.; Kokke, W.; Refaeli, I.; Amir, G.; Julian, K.; Bassan, S.; et al. 2024. Marabou 2.0: A Versatile Formal Analyzer of Neural Networks. Technical Report. <https://arxiv.org/abs/2401.14461>.
- Yerushalmi, R.; Amir, G.; Elyasaf, A.; Harel, D.; Katz, G.; and Marron, A. 2022. Scenario-Assisted Deep Reinforcement Learning. In *Proc. 10th Int. Conf. on Model-Driven Engineering and Software Development (MODELSWARD)*, 310–319.
- Yerushalmi, R.; Amir, G.; Elyasaf, A.; Harel, D.; Katz, G.; and Marron, A. 2023. Enhancing Deep Reinforcement Learning with Scenario-Based Modeling. *SN Computer Science* 4(2):156.
- Yu, G.; Lee, J.; and Bae, K. 2022. Stlmc: Robust STL model checking of hybrid systems using SMT. In *Proc. of the 34th International Conference in Computer Aided Verification (CAV(2022), Part I*, volume 13371 of *LNCS*, 524–537. Springer.
- Zamora, I.; Lopez, N.; Vilches, V.; and Cordero, A. 2016. Extending the Openai Gym for Robotics: a Toolkit for reinforcement Learning Rsing Ros and Gazebo. *arXiv preprint arXiv:1608.05742*.
- Zhang, H.; Weng, T.; Chen, P.; Hsieh, C.; and Daniel, L. 2018. Efficient Neural Network Robustness Certification with General Activation Functions. In *Proc. 31st Conf. on Neural Information Processing Systems (NeurIPS)*, 1097–1105.

Zhang, J.; Kim, J.; O’Donoghue, B.; and Boyd, S. 2020. Sample Efficient Reinforcement Learning with REINFORCE. Technical Report. <https://arxiv.org/abs/2010.11364>.

Zhu, Y.; Mottaghi, R.; Kolve, E.; Lim, J.; Gupta, A.; Fei-Fei, L.; and Farhadi, A. 2017. Target-Driven Visual Navigation in Indoor Scenes Using Deep Reinforcement Learning. In *Proc. 2017 IEEE Int. Conf. on Robotics and Automation (ICRA)*.

A First-Order Theories

Due to lack of space, we have not been able to define the first-order theories extensively in Sec. 2, so we show their formalisation and details below.

Definition. We use sorted first-order theories for extending the expressivity of the atomic predicates. For our purposes, a (sorted) first-order theory \mathcal{T} consists of (1) a first-order vocabulary to form terms and predicates, (2) an interpretation of the domains of the sorts, and (3) an automatic reasoning system to decide the validity of sentences in the theory. A first-order theory \mathcal{T} (see e.g., (Bradley and Manna 2007)) is given by its signature Γ , which is a set of constant, function, and predicate symbols. A Γ -formula is constructed from constant, function, and predicate symbols of Γ , together with logical connectives and quantifiers. The symbols Γ are symbols without prior meaning that are later interpreted.

A Γ -formula φ is valid in the theory \mathcal{T} (i.e., φ is \mathcal{T} -valid), if for every interpretation I that satisfies the axioms of \mathcal{T} , then $I \models \varphi$. We write $\mathcal{T} \models \varphi$ to mean that φ is \mathcal{T} -valid. Formally, the theory \mathcal{T} consists of all closed formulae that are \mathcal{T} -valid, where *closed* means that all the variables are quantified in the formula. A Γ -formula φ is satisfiable in \mathcal{T} (i.e., \mathcal{T} -satisfiable), if there is a \mathcal{T} -interpretation I that satisfies φ .

A theory \mathcal{T} is decidable if $\mathcal{T} \models \varphi$ is decidable for every Γ -formula φ . That is, there is an algorithm that always terminates with \top if φ is \mathcal{T} -valid or with \perp if φ is \mathcal{T} -invalid.

Arithmetic theories A particular class of first-order theories is that of arithmetic theories, which are well studied in mathematics and theoretical computer science, and are of particular relevance in formal methods. Most of these theories are decidable. In this paper, we use three of them:

- *Linear Integer Arithmetic* $\mathcal{T}_{\mathbb{Z}}$ the theory of integer numbers with addition but no arbitrary multiplication. The signature is $\Gamma_{\mathbb{Z}} = \{\dots, -1, 0, 1, \dots, +, -, =, >\}$. An example of a literal is $(2x > -4)$.
- *Linear Rational/Real Arithmetic* $\mathcal{T}_{\mathbb{Q}}$: the theory of real/rational numbers with addition but no arbitrary multiplication. The signature is $\Gamma_{\mathbb{Q}} = \{0, k, +, -, =, >\}$, where $k \in \mathbb{Q}$. For instance, a literal is $(2x > -\frac{1}{3})$.
- *Nonlinear Real Arithmetic* $\mathcal{T}_{\mathbb{R}}$ is the theory of real numbers with both addition and arbitrary multiplication. The signature is $\Gamma_{\mathbb{R}} = \{0, k, +, -, =, >, \cdot\}$. An example of a literal is $(2x^2 > \frac{1}{3})$.

Note that a theory of (linear) naturals $\mathcal{T}_{\mathbb{N}}$ is subsumed by $\mathcal{T}_{\mathbb{Z}}$ and a theory of (non-linear) complex numbers is subsumed by $\mathcal{T}_{\mathbb{C}}$.

Fragments of \mathcal{T} . A fragment of a theory is a syntactically-restricted subset of formulae of the theory. For example, the quantifier-free fragment of a theory \mathcal{T} is the set of formulae without quantifiers that are valid in \mathcal{T} . A fragment of \mathcal{T} is decidable if $\mathcal{T} \models \varphi$ is decidable for every Γ -formula φ in the fragment.

In this paper, we considered theories \mathcal{T} whose $\exists^*\forall^*$ fragment is decidable, which not only considers arithmetic theories, but many others such as, the array property fragment (Bradley, Manna, and Sipma 2006), which is decidable for the $\exists^*\forall_{\mathbb{Z}}$ fragment. Indeed, many others theories beyond numerical domains span from Bernays–Schönfinkel–Ramsey (BSR) class (Fontaine 2007), which is less expressive than the general $\exists^*\forall^*$ -fragment considered in this paper. For instance, (Reynolds, Iosif, and Serban 2017) shows decidability of the fragment of first-order separation logic (SL) restricted to BSR where the quantified variables range over the set of memory location; however, SL becomes undecidable when the quantifier prefix belongs to $\exists^*\forall^*\exists^*$.

B Deep Neural Networks and Verification

B.1 Deep Neural Networks (DNNs)

A DNN (Goodfellow, Bengio, and Courville 2016) is a directed, computational graph, consisting of a sequence of layers. The DNN is evaluated by propagating its input values, layer-by-layer, until reaching the final (output) layer. The computed output values can be interpreted as a regression value, or a classification, depending on the type of the DNN in question. The computation itself depends also on the *type* of the DNN’s layers. For example, a node z in a *rectified linear unit (ReLU)* layer calculates the value $z = \text{ReLU}(x) = \max(x, 0)$, for the value x of one of the nodes among the preceding layers. Other layer types include *weighted sum* layers (that compute an affine transformation), and various layers with non-linear activations. As in most prior work on DNN verification, we focus on DNNs in which every layer is connected exclusively to its following layer; these general architectures are termed *feed-forward* neural networks, and are extremely popular. A toy (regression) DNN is depicted in Fig. 3. For an input vector $V_1 = [1, 2]^T$, the values $V_2 = [10, -5]^T$ are computed by the second layer. Subsequently, in the third layer, ReLU activations are applied, producing the vector $V_3 = [10, 0]^T$. Finally, the single output value of the network is $V_4 = [10]$.

B.2 Deep Reinforcement Learning

In this paper, we focus on Deep Reinforcement Learning (DRL) (Li 2017; Sutton and Barto 2018), which is a popular paradigm in the *unsupervised learning* setting, for training DNNs, in which the DNN agent learns from *experience*, instead of *data*. Specifically, the agent is iteratively trained to learn a policy π , mapping every environment state s (observed by the agent) to an appropriate action a . The learnt policy has various interpretations across different training

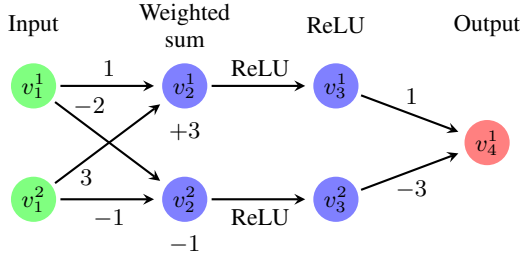


Figure 3: A toy DNN.

algorithms (Zhang et al. 2020; Van Hasselt, Guez, and Silver 2016; Schulman et al. 2017). For example, in some cases, π may represent a probability distribution over the possible actions, while in other cases it may encode a function estimating a desirability metric over all future actions from a given state s . DRL agents are pervasive among various safety-critical domains, and especially, among robotic systems (Marchesini and Farinelli 2020; Marchesini, Corsi, and Farinelli 2021a; Marchesini, Corsi, and Farinelli 2021b; Pore et al. 2021).

B.3 DNN Verification

A DNN verification engine (Katz et al. 2017; Gehr et al. 2018; Wang et al. 2018; Lyu et al. 2020; Huang et al. 2017; Marzari et al. 2023) receives as inputs: a DNN N , a precondition P over the network’s inputs, and a postcondition Q limiting the network’s outputs. The verification engine searches for an input y satisfying the property $P(y) \wedge Q(N(y))$. If there exists such an input, a SAT result is returned, along with a concrete input z satisfying the constraints; otherwise, UNSAT is returned, indicating that no such input exists. Typically, the postcondition Q specifies the *negation* of the desired property, and thus a SAT result implies that the property is violated, with the returned z being an input that triggers a bug. However, an UNSAT result implies that the (desired) property holds throughout the input space.

Marabou. In this work, the DNN verification procedure was executed by *Marabou* (Katz et al. 2019), a popular verification engine that has achieved state-of-the-art results on a wide variety of DNN benchmarks (Amir et al. 2023a; Amir et al. 2021).

Example. For instance, if we were to check whether the DNN depicted in Fig. 3 always outputs a value larger than 7; i.e., for any input $x = \langle v_1^1, v_1^2 \rangle$, then $N(x) = v_4^1 > 7$. This property can be encoded as a verification query with a precondition that does not restrict the inputs, i.e., $P = (\text{true})$, and by setting the postcondition $Q = (v_4^1 \leq 7)$. For this query, a sound verification engine will return a SAT answer, alongside a feasible counterexample, e.g., $x = \langle 2, 0 \rangle$, which produces $v_4^1 = 7 \leq 7$, proving that this property does not hold for the DNN in question.

Complexity. It has been shown that the process of sound and complete verification of a given DNN with ReLU activations

is ‘NP-complete’. Hence, even a linear growth to the size of a DNN (i.e., the total number of weights and neurons) can cause in the worst-case scenario, an exponential blowup in verification runtime. This complexity was deduced by Katz et al. (Katz et al. 2017), by presenting a polynomial-time reduction from the popular 3-SAT problem, known to be NP-complete. We note however, that there exist various heuristics that allow to efficiently prune the search space and reduce the overall verification time in many cases (Amir et al. 2021; Katz et al. 2019).

B.4 Comparing Shielding with DNN Verification

DNN verification is the classic alternative approach to shielding. In the DNN verification setting, we train a collection of models, and check independently whether each model obeys all required properties. After the verification process, we hope to retain a model that will behave correctly.

General Comparison. Next, we will cover the main advantages and setback on using each of these two competing approaches:

1. **Activation Functions and Model Expressivity.** Marabou and most DNN verification engines can verify only piecewise-linear constraint. Hence, this significantly limits the *type* of DNN being verified, as well as the property in question. Shields, on the other hand, treat DNN as a black box input/output system, and are agnostic to the expressivity level of the DNN in question. In addition, our shielding approach is limited solely to the expressivity of arbitrary LTL formulas.
2. **Verification Runtime.** Another advantage of shields is that they are significantly faster to implement when compared to DNN verification. This for two reasons. First, a single shield can be used for all DRL agents and all properties, while an SMT-based verification engine, for example, must verify each property separately, per each separate agent. To demonstrate this point, we verified 7 properties per each of the 700 DRL agents trained on the TurtleBot benchmark. This resulted in 4,900 unique verification queries (one per each DRL agent, and per each property). In addition to verification finding violations (i.e., SAT assignments) for *all* properties, the accumulative runtime with Marabou was over 1,935 seconds (!), when running also with a state-of-the-art *Gurobi* solver (Optimization 2021). These results are depicted in Fig. 4.
3. **Pervasiveness.** On the other hand, a clear advantage of DNN verification, relative to shielding, is that DNN verification can be executed *offline*. Thus, given that DNN verification identifies a correct model, it can be deployed safely into the wild, without and pervasive intervention of additional sources. Shielding on the other hand, constantly requires monitoring of the decisions of a given DRL system.
4. **System Soundness.** Finally, we note that given a DNN verification engine identifies a successful agent, we can rely with high confidence on the, original, decided actions — otherwise, an incorrect action that would have violated

a property, should be identified beforehand with verification. Shielding, on the other hand, constantly requires overriding the unwanted behavior, and hence possibly enforcing an action that can be sub-optimal.

Note. It is still worth mentioning that there are no formal guarantees that a single DNN agent will indeed “survive” the formal-verification-driven filtering process. For example, in all 4,900 verification queries described in Fig. 4, all 700 agents were found to violate all properties, at least in a single scenario. We believe that these empirical results further motivate the need for shielding.

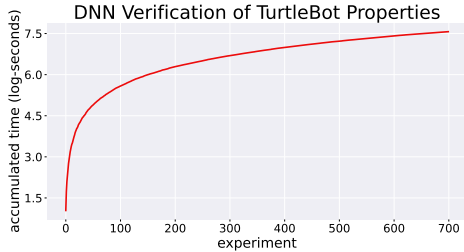


Figure 4: Total accumulated time (in log-scale) for all 4,900 experiments, all of which include violations of the properties of interest.

Complexity Comparison. As the complexity of our shielding approach is dominated by the complexity of LTL synthesis, it is 2EXPTIME-complete in general. In practice, however, many LTL fragments tend to be synthesized in a runtime process that is significantly more efficient than this worst-case complexity; e.g., GR(1), GX0, etc. But most importantly, the NP-completeness is not on the same measure of size (i.e., total neurons of the DNN) than the LTL formula, which is significantly smaller, in practice. DNN verification on the other hand, is NP-complete (Katz et al. 2017), as a function of the size of the DNN in question, i.e., the total number of DNN parameters. We note that a direct comparison between complexities of shielding and DNN verification is not straightforward, as each depends on a different type of input (size of the LTL formula vs. the total number of DNN parameters).

C Details about the GridWorld case study

Properties. Specifically, we classified the *wanted* behaviours into two categories:

- **Safety:** decisions that cause the agent to collide in the next time-step. *For example, when the agent is near an obstacle on the left, then it should not select the action LEFT.* These properties show that, given all the necessary properties, we can avoid collision in all executions.
- **Liveness:** decisions that do not cause the robotic to collide in the next time-step but generate an infinite loop. *For example, when the robot iteratively performs a sequence of actions that brings it to the same position (e.g., RIGHT, LEFT, and RIGHT).* These properties show that our shields can manage dynamics.

Note that, although these requirements can look straightforward to accomplish for a state-of-the-art D , the random noise can potentially generate really specific input configuration, known as *adversarial inputs*, that can easily fool the neural network to perform unexpected and unexplainable actions (Kazak et al. 2019).

DRL and Training Results GridWorld is a classical problem for reinforcement learning, and many previous works efficiently solve it with many state-of-the-art solutions and algorithms. However, our modified version with the addition of a random noise to the agent readings, makes the task drastically more challenging. We design a neural network to match the state and observation space of the environment and employ a simple neural feed-forward neural network, consisting of *layers* of 32 neurons each, activated with the popular ReLU function. In more detail:

1. An *input layer* of 8 neurons. The first 2 inputs represent the coordinates of the agent in the grid, these inputs can assume continuous values given the addition of the Gaussian noise. The next 4 neurons represent a *proximity sensor* that indicates whether the agent has an obstacle in one of the 4 possible directions. The last 2 input feature encodes the coordinates of the target.
2. An *output layer* of 4 neurons, one for each direction (i.e., UP, LEFT, RIGHT, and DOWN). The agent always performs the action corresponding to the output node with the highest value.

We trained our agents with the state-of-the-art *Proximal Policy Optimization* (PPO) algorithm (Schulman et al. 2017), which has shown promising results in a large variety of tasks. A crucial component of effective training is the reward function. For this task, we employ a discrete reward function, in detail:

$$r_t = \begin{cases} 1 & \text{if the target is reached} \\ -5 & \text{if the agent collides} \\ -0.01 & \text{otherwise} \end{cases} \quad (1)$$

notice that we employ a small penalty of -0.01 for each time step to push the agent toward finding the shortest path.

D A TurtleBot case study

D.1 Expressivity in \mathcal{T}

Case Study: Robotic Navigation Systems. *Clearpath Turtlebot 4* (TB), depicted in Fig. 5, is a widely adopted platform in the field of robotics research (Nandkumar, Shukla, and Varma 2021; Ruan et al. 2019; Zamora et al. 2016), given its versatility and applicability to real-world systems. Specifically, we focus on the *mapless navigation* variant, in which the robot (controlled by a DRL agent) learns to navigate throughout an unknown arena, relying on its lidars and other, local sensors (Marchesini and Farinelli 2020; Zhu et al. 2017). For more details, see App. D.

Partial Observability. We continue to focus on *collision avoidance* properties. However, unlike the case with GW

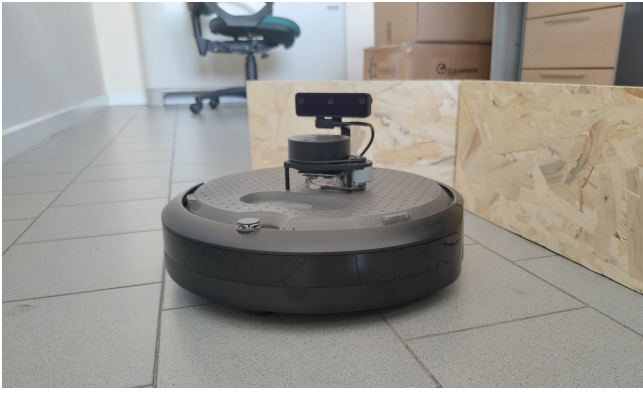


Figure 5: The Clearpath Turtlebot 4 platform.



Figure 6: The average success rate obtained by our DRL-trained agents.

(Subsec. 4.1 the current environment is only *partially observable*. More formally, when using $S_{\mathcal{T}}$ we do not possess a complete transition model of both players. Hence, $S_{\mathcal{T}}$ can only guarantee $\varphi_{\mathcal{T}}$, but not *high-level* behavioural properties, e.g., *collision avoidance*. However, TB demonstrates that our approach allows encoding complex properties also in this harder and realistic setting. This is possible due to Thm. 1, which implies that $S_{\mathcal{T}}$ enforces $\varphi_{\mathcal{T}}$ based on many theories \mathcal{T} , including non-linear real arithmetic.

Empirical Evaluation. We trained a pool of 700 models, differing in the random seed used to generate them. The models reached a high success threshold of 98% (see Fig. 6). For additional details regarding the training procedure, see App. D.3. Although these models attained a high success rate; when simulated, we identified various edge cases in which they behaved unsafely. We note that these unwanted behaviors appeared even after additional, extensive training rounds. To further demonstrate our shield, we employed it to guarantee various types of *wanted* behavior of TB, under user-defined specifications:

- **Safe:** actions that do not cause the robot to collide in the next time-step. *For example, when the robot is near an obstacle, then it should not move towards it.*
- **Predictable:** actions that do not result to potentially unexpected outcomes. *For example, the agent should avoid rapidly and simultaneously increasing both its angular*

velocity and its linear velocity.

- **Efficient:** actions that are optimal under the given circumstances. *For example, if the target can be safely reached in very few time-steps, the agent should avoid unnecessarily long trajectories.*

We encoded violations of five different types of safety properties ($S1$, $S2$, $S3$, $S4$, and $S5$), two types of violations for predictable behaviors ($P1$ and $P2$), and a violation of a single type of required efficient behavior ($E1$). Concretely, $D \cdot S_{\mathcal{T}}$ will output values in non-linear real arithmetic; e.g., $S5$ is $\neg[(x_4 - 0.17 < y_0 \cdot 0.015) \wedge (y_1 > 0.15)]$, etc. A full encoding of all properties appears in App. D.4.

Results. To analyze our approach, we randomly sampled 1000 trajectories with various actions (some ending with a collision, and some reaching the target safely). Next, we constructed $S_{\mathcal{T}}$ to guarantee the following property combinations: spe (safe, predictable, and efficient), sp (safe and predictable), se (safe and efficient), and s (safe). Our experiments demonstrated that $S_{\mathcal{T}}$ synthesis was indeed able to detect unrealizable specifications. Also, when the specification was realizable, the synthesis runtime was extremely fast — with all shields generated in less than 7.81 seconds.

Next, we randomly selected 10 traces (half successful, and half not), and conducted an in-depth analysis of the behavior of our $S_{\mathcal{T}}$ — both in terms of runtime, and in terms of overriding actions. Specifically, we aim to (1) show non-linear outputs and (2) understand how the combinations of various properties can affect runtime and corrections. Our results are summarized in Tab. 3, and include, per each trace (row) and property combination (column), the mean execution time (T_m) for generating $S_{\mathcal{T}}$, as well as the ratio of overwritten actions (O), out of all actions in total (T). First, we analyzed how the addition of properties affects the overall behavior of the shield. Indeed, the results behaved as expected — the more properties that were enforced ($s \rightarrow sp, se \rightarrow spe$) the less permissive $S_{\mathcal{T}}$ was, i.e., the higher the O/T ratio was, as there were more “wrong” behaviors to correct. Another observed behavior is that, in most cases, the more properties that $\varphi_{\mathcal{T}}$ encoded, the more time it took for $S_{\mathcal{T}}$ to override actions. This too, was not surprising, as more properties are translated to more constraints considered by the underlying SMT solver. Our analysis also raised some surprising results. For example, by comparing property combinations sp and se , it is evident that there is a vast difference between the success in learning various properties. For example, the shields tend to intervene significantly more when enforcing “predictable” behavior, than when enforcing “efficient” behavior. The fact that “efficient” decisions are corrected much less (especially in failure traces) suggests that these behaviors are learned more successfully during training. This also demonstrates how shielding can be used not only for guaranteeing correctness, but for understanding the generalization of these “black box” DRL artifacts. Also, we can observe overall a considerable amount of actions overridden by $S_{\mathcal{T}}$ in almost all experiments, even though the robot is controlled by highly-successful DRL

agents. We believe that this further demonstrates the merits of our approach. For additional details, see App. D.

D.2 DRL and Training Results

State-of-the-art solutions suggest that it is possible to train an effective agent by exploiting simple neural architecture. In particular, we took inspiration from the topology presented in previous related work (Marchesini and Farinelli 2020; Amir et al. 2023a) that consists of a modest feed-forward DRL, consisting of two hidden layers of 32 neurons each, with the popular ReLU activation units. As our DRL is a regression (and not a classification) network, we were able to directly encode continuous actions in the output layer, hence allowing the DRL agents to potentially encode any possible action in the state space. More formally, we summarize the network’s topology as follows:

1. An *input layer* of 9 neurons. The first 7 inputs represent lidar sensor readings, that indicate the distance from an obstacle in a given direction (from left to right, with a step of 30°); the last two input nodes represent the local position of the target in polar coordinates (i.e., angle and distance).
2. Two fully connected *hidden layers* of 32 neurons, with ReLU activations.
3. An *output layer* of 2 neurons. The first neuron returns the linear velocity (i.e., the speed of the robot), and the second one provides the angular velocity (i.e., a single value indicating the rotation). These two values together allow to directly evaluate the location of the robot in the next time step.

We trained our agents with the state-of-the-art *Proximal Policy Optimization* (PPO) algorithm (Schulman et al. 2017), which has shown promising results in a large variety of tasks, specifically, in robotics navigation. A crucial component of effective training is the reward function. In this work, we exploited a continuous reward, with the addition of discrete bonuses to encourage (or discourage) specific behaviors. More formally, the reward (R_t) during time-step t of the training phase is defined as follows:

$$R_t = \begin{cases} \pm 1 & \text{terminal states} \\ (dist_{t-1} - dist_t) \cdot \eta - \beta & \text{otherwise} \end{cases} \quad (2)$$

Where $dist_k$ is the distance from the target at time k ; η is a normalization factor; and β is a penalty, designed to encourage the robot to reach the target quickly (in our experiments, we empirically set $\eta = 3$ and $\beta = 0.001$). Additionally, in terminal states, we increase the reward by 1 if the target is reached, or decrease it by 1 in case of collision.

D.3 Training Details

Now we discuss the hyperparameters for training and various implementation details for TurtleBot.

General Parameters

- *training episodes*: 500
- *number of hidden layers*: 2

- *size of hidden layers*: 32
- *parallel environments*: 1
- *gamma* (γ): 0.99
- *learning rate*: 0.0003

We followed the insights from (Marchesini and Farinelli 2020) for the network topology (see Sec.D.1 of the main paper). However, a crucial difference, between our setting and the one appearing in (Marchesini and Farinelli 2020), is that our agents have two continuous outputs, instead of five discrete possible actions; this provides our agent with a higher expressiveness level.

PPO Parameters For the advantage estimation and the critic update, we rely on the generalized advantage estimation strategy (GAE). The update rule follows the guidelines of the *OpenAI’s Spinning Up* documentation.⁵ Following is a complete list of the hyperparameters for our training:

- *memory limit*: None
- *update frequency*: 4096 steps
- *trajectory reduction strategy*: sum
- *actor epochs*: 50
- *actor batch numbers*: 16
- *critic epochs*: 60
- *critic batch numbers*: 32
- *critic network size*: 2x256
- *PPO clip*: 0.2
- *GAE lambda*: 0.95
- *target kl-divergence*: 0.02
- *max gradient normal*: 0.5

Random Seeds for Reproducibility: finally, we present a complete list of the random seeds we used for the training: [84, 234, 256, 403, 597, 634, 732]. These seeds are applied to the following Python modules: *Random*, *NumPy*, and *PyTorch*. We plan on making our experiments publicly available in the final version of this paper.

D.4 Requirements Formalization

The first 7 inputs of the network (i.e., the lidar scans) are normalized in the range $[0, 1]$, where 0 means that the obstacle is at the minimum distance and 1 means that the path is free in the required direction; the input number 8 (i.e., distance from the target) is normalized between 0 and 1 on the size of the map; finally, the last input (i.e., the angle for the polar coordinates) is normalized between 0 (target on the left) and 1 (target on the right).

However, given the following consideration, we found that these standard bounds can be further tightened: (i) the true lower-bound for a lidar scan can be increased to a value of 0.03 to guarantee a minimal room for rotating the robot; (ii) the proportion between the distance from an obstacle and the maximum linear velocity that allows a safe collision

⁵<https://spinningup.openai.com/en/latest/>

Trace	spe			sp			se			s		
	Tm.	O/T	%	Tm.	O/T	%	Tm.	O/T	%	Tm.	O/T	%
00.00	64	172/288	59.7	59	77/288	26.7	61	142/288	49.3	57	47/288	16.3
00.06	60	86/225	38.2	60	62/225	27.5	58	75/225	33.3	57	51/225	22.6
00.08	64	109/268	40.6	61	101/268	37.6	59	65/268	24.2	57	57/268	21.2
01.01	66	119/206	57.7	61	96/206	46.6	59	70/206	33.9	57	47/206	22.8
01.02	64	133/342	38.8	62	129/342	37.7	63	56/342	16.3	52	52/342	15.2
00.07	76	21/21	100.0	74	21/21	100.0	72	21/21	100.0	71	21/21	100.0
13.07	70	29/54	53.7	68	29/54	53.7	67	13/54	24	67	13/54	24
29.02	73	7/9	77.7	72	7/9	77.7	66	2/7	28.5	64	2/7	28.5
48.05	63	70/372	18.8	62	70/372	18.8	59	34/372	9.1	61	34/372	9.1
59.07	68	15/51	29.4	69	15/51	29.4	63	7/51	13.7	67	7/51	13.7

Table 3: For each trace and property combination, we present the average S_T intervention time and number of corrections (first 5 traces are successful, and the last 5 traces are not). Time is measured in milliseconds.

avoidance is a factor $\alpha = 0.015$ (the following encoding shows the effect of this parameter); and (ii) to avoid configurations in which the agent can solve the task in less than 3 steps, we set a minimum distance from the target of 0.2.

Complete list of constraints and requirements: notice that all the following properties are encoded as unwanted behaviors, i.e., something that the agent should NOT do. Notice that with X we represent the input nodes and with Y the outputs.

- SAFETY 1 (S1): avoid collision with an obstacle in front of the robot.
 - $X[3] - 0.17 < Y[0] \cdot 0.015$
- SAFETY 2 (S2): avoid collision with an obstacle on the left of the robot.
 - $(X[1] - 0.17 < Y[0] \cdot 0.015)$ and $(Y[1] < -0.2)$
- SAFETY 3 (S3): avoid collision with an obstacle *slightly* on the left of the robot.
 - $(X[2] - 0.17 < Y[0] \cdot 0.015)$ and $(Y[1] < -0.15)$
- SAFETY 4 (S4): avoid collision with an obstacle on the right of the robot.
 - $(X[5] - 0.17 < Y[0] \cdot 0.015)$ and $(Y[1] > 0.2)$
- SAFETY 5 (S5): avoid collision with an obstacle *slightly* on the right of the robot.
 - $(X[4] - 0.17 < Y[0] \cdot 0.015)$ and $(Y[1] > 0.15)$
- PREDICTABLE 1 (P1): avoiding a strong rotation if the robot is accelerating.
 - $Y[1] > 3 \cdot Y[0]^2$
- PREDICTABLE 2 (P2): avoiding a strong acceleration while the robot is rotating.
 - $abs(Y[1]) > 0.7$ and $Y[0] > 0.7$

- EFFICIENT 1 (E1): avoid turning if the goal is in front of the robot and there are no obstacles in that direction.
 - $X[1] > 0.45$ and $X[7] < 0.55$ and $X[3] == 1$ and $Y[1] > 0.05$

D.5 Evaluation: Component-level Runtime Analysis.

Moreover, we checked in a higher resolution which of the shield’s components are the most resource-consuming. We selected another collection of 20 traces, for which we measured the synthesis time of the underlying components: partitioner (Pa.), Boolean controller (Cn.) and provider (Pr.). The results (summarized in Tab. 4) suggest that the partitioner is the component that takes the most time (about 0.04 seconds). This is probably due to the current partitioner implementation which relies on an exhaustive algorithm to do so. We acknowledge that the implementation of Pa. and Pr. is made in Python, whereas Cn. is an external component `aigsim`⁶ in C, so shield performance would benefit from any advance in such implementations. Note that the amount of intervention of the shield is high because we are considering safety, dangerous, and behavioral properties. Also, note that this amount is usually higher than 80% when the trace represents a trajectory in which the agent failed to reach the target.

⁶See: <https://github.com/arminbiere/aiger/>

Trace	Component times			Overall measures		
	Pa.	Cn.	Pr.	Ex.	O/T	%
00	0.019	1.187(5)	0.016	3.160	13/88	14.77
01	0.041	1.943(6)	0.019	29.038	334/478	69.87
02	0.041	4.213(6)	0.017	22.397	186/379	49.07
03	0.043	4.251(6)	0.018	22.659	289/367	78.74
04	0.038	3.573(6)	0.018	11.851	149/207	71.98
05×	0.049	1.299(5)	0.017	8.659	112/128	87.50
06×	0.050	5.613(6)	0.018	8.261	107/119	89.91
07×	0.048	1.783(6)	0.017	29.420	200/448	44.64
08	0.033	6.460(6)	0.017	7.392	78/143	54.54
09	0.017	1.017(5)	0.015	2.806	0/82	0.00
10	0.042	4.251(6)	0.017	19.641	150/330	45.45
11×	0.049	2.690(5)	0.018	19.641	49/49	100.00
12	0.039	3.193(6)	0.017	13.472	139/233	59.65
13×	0.033	3.648(6)	0.018	14.556	225/279	80.65
14	0.040	3.785(6)	0.016	14.866	90/260	34.61
15	0.040	5.678(6)	0.017	16.513	221/283	78.09
16×	0.042	2.478(6)	0.018	14.556	415/606	68.48
17	0.044	5.238(6)	0.018	32.910	288/522	55.17
18	0.018	6.568(6)	0.015	3.465	0/100	0.00
19×	0.050	8.744(6)	0.018	5.981	87/87	100.00

Table 4: Time-wise performance of components. “X” in the first columns indicates the trace represents a failed trajectory. (Ex.) measures the execution time for the whole trace.